

**GLASS FIBER REINFORCED NANOCOMPOSITES –  
EFFECTS OF FIBER ORIENTATION AND NANOCLAY  
CONTENT**

**A  
Thesis Report**

**submitted in partial fulfilment of the requirement for the award of degree**

**MASTER OF ENGINEERING  
in  
PRODUCTION & INDUSTRIAL ENGINEERING**

**Submitted By**

**VikasDagar**

**(Roll No. 820982004)**

**Under Guidance of**

**Mr. BIKRAMJIT SHARMA  
Assistant Professor  
Deptt. of Mechanical Engg.  
Thapar University, Patiala**

**Dr. RAJEEV MEHTA  
Associate Professor & Head  
Deptt. of Chemical Engg.  
Thapar University, Patiala**



**MECHANICAL ENGINEERING DEPARTMENT  
THAPAR UNIVERSITY, PATIALA-147004, INDIA**

(Declared as Deemed-to-be university u/s 3 of the UGC Act, 1956)

## CERTIFICATE

---

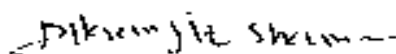
This is to certify that the work in this thesis report "Glass fiber reinforced nanocomposites effects of fiber orientation and nanoclay content" submitted in partial fulfilment of requirement for the award of **Master of Engineering Degree in Production & Industrial Engineering** in Mechanical Engineering Department, Thapar University, Patiala, is an authentic record of work carried out by me under the guidance of Mr. Bikramjit Sharma, Assistant Professor, Mechanical Engineering Department, Thapar University, Patiala and Dr. Rajeev Mehta, Associate Professor & Head, Chemical Engineering Department, Thapar University Patiala.

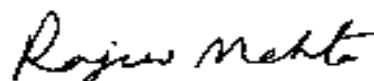
The matter embodied in this report has not been submitted in part or full to any university or institute for the award of any degree.

Date: 07.01.2013

  
(VIKAS DAGAR)

This is to certify that the above declaration made by the student is correct to the best of my knowledge and belief.

  
**Mr. BIKRAMJIT SHARMA**  
Assistant Professor  
Deptt. of Mechanical Engg.  
Thapar University, Patiala

  
**Dr. RAJEEV MEHTA**  
Associate Professor & Head  
Deptt. of Chemical Engg.  
Thapar University, Patiala

Countersigned by:

  
**Dr. AJAY BATISH**  
Professor & Head  
Deptt. of Mechanical Engg.  
Thapar University, Patiala

  
**Dr. S.K. MOHAPATRA**  
Dean of Academic Affairs  
Thapar University, Patiala

## **ACKNOWLEDGEMENT**

---

I am highly grateful to the authorities of Thapar University, Patiala for providing the opportunity to carry out this thesis work.

I would like to express a deep sense of gratitude and thank profusely to my thesis guide **Mr. Bikramjit Sharma**, Assistant Professor, Mechanical Engineering Department and **Dr. Rajeev Mehta**, H.O.D, Chemical Engineering Department for their sincere & invaluable guidance and suggestions which inspired me to submit thesis report in the present form.

I am highly thankful to **Mr. Toesh** (Ph.D Scholar in Chemical Engineering Department) for his continuous support and helping in conducting tensile & flexural testing.

I heartily thank to **Mr. Jagtar Singh** and **Mr. Dinesh Kumar Sharma** (P.U. Chandigarh) for helping me in conducting the tests on TEM and XRD tests.

I heartily thank to **Mr. Kushal Sen**, Coordinator, SEM Central Facility, Textile Technology Department, IIT Delhi for helping me in conducting the SEM test.

I am also thankful to other faculty members and all the workshop staff of Mechanical Engineering Department and Chemical Engineering Department, Thapar University, Patiala for their support.

I would also like to thank and acknowledge **BASF Construction Chemicals (India) Private Limited** and **Connell Bros. Mumbai** for supplying us generously with E-Glass Fibre sheet, M Brace epoxy (Base and hardener) and Clay (Closite 30B) etc. for this experimentation.

My special thanks are due to my family members and friends who constantly encouraged me to complete this study.

  
**VIKASDAGAR**

## ABSTRACT

---

The introduction of nanosized reinforcements in polymer matrix at low concentration results in improvement in properties of fiber reinforced composites. The main challenges involved to obtain improved properties are (1). Uniform dispersion of nanosized reinforcement in matrix and (2). Good adhesion between the reinforcements and matrix. In the nanoclay based nanocomposites, the exfoliation of nanoclay along with uniform dispersion and adhesion leads to much improved composites with same fiber content. In the present work, mechanical and morphological properties of E glass fiber reinforced epoxy nanoclay composites have been studied by varying the nanoclay content and fiber orientation. Cloisite 30B<sup>®</sup> nanoclay was mixed in epoxy at two different concentrations (2 wt% and 3wt%) and the modified matrix was used to synthesize E glass fiber epoxy composites having 30<sup>0</sup>, 45<sup>0</sup> and 60<sup>0</sup> fiber orientation using hand layup method. The baseline data for comparison was generated by carrying out tests on neat epoxy glass fiber composites. The incorporation of Cloisite 30B nanoclay increased the flexural and tensile strength of the fiber reinforced composites significantly. The flexural strength of E glass fiber epoxy composite increased by 22.62% and the tensile strength increases by 10.57% with a 3 wt% nanoclay addition. This result is due to the exfoliation of Cloisite 30B<sup>®</sup> nanoclay in the epoxy matrix. The improvement in the properties may be attributed to the high aspect ratio, contact surface and reinforcing effects of the nanoclay.

# INDEX

<b>S.No.</b>	<b>TITLE</b>	<b>PAGE No.</b>
	<b>CERTIFICATE</b>	ii
	<b>ACKNOWLEDGEMENT</b>	iii
	<b>ABSTRACTS</b>	iv
	<b>INDEX</b>	v-vi
	<b>LIST OF FIGURES</b>	vii-viii
	<b>LIST OF TABLES</b>	ix
<b>CHAPTER 1</b>		
	<b>INTRODUCTION</b>	
1.1	<b>NANOTECHNOLOGY</b>	1
1.2	<b>NANOCOMPOSITES</b>	1
1.3	<b>CLASSIFICATION OF NANOCOMPOSITES</b>	2
1.3.1	<b>CERAMIC MATRIX NANOCOMPOSITES</b>	3
1.3.2	<b>METAL MATRIX NANOCOMPOSITES</b>	4
1.3.3	<b>POLYMER MATRIX NANOCOMPOSITES</b>	4-9
1.4	<b>GLASS FIBER</b>	9-11
1.5	<b>EPOXY RESIN</b>	11
1.6	<b>FIBER REINFORCED EPOXY/CLAY NANOCOMPOSITE</b>	11
<b>CHAPTER 2</b>		
	<b>LITRATURE REVIEW</b>	12-20

<b>CHAPTER 3</b>		
3.1	GAPS IN LITRATURE REVIEW	21
3.2	RESEARCH PROBLEM	21
3.3	OBJECTIVES	21
<b>CHAPTER 4</b>		
FABRICATION AND EXPERIMENTATION		
4.1	METHODOLOGY	22
4.2	FABRICATION OF SPECIMEN	23-28
4.3	TESTING METHODS USED IN EXPERIMENTATION	28-33
<b>CHAPTER 5</b>		
RESULTS AND DISCUSSIONS		
5.1	MICROSCOPIC BEHAVIOR	34
5.1.1	MICRO HARDNESS	34-35
5.1.2	X-RAY DIFFRACTION TEST	35-36
5.1.3	SCANNING ELECTRON MICROSCOPE (SEM)	37
5.1.4	TRNASMISSION ELECTRON MICROSCOPY(TEM)	38-39
5.2	FLEXURAL BEHAVIOUR	39-43
5.3	TENSILE BEHAVIOUR	43-47
<b>CHAPTER 6</b>		
CONCLUSION AND FUTURE SCOPE		
6.1	CONCLUSION	48
6.2	FUTURE SCOPE	48
<b>REFERENCES</b>		49-50

## LIST OF FIGURES

<b>Figure No.</b>	<b>Title</b>	<b>Page No.</b>
Fig.1.1	Classification of Nanocomposites:based on matrices	3
Fig.1.2	Schematic representation of basic types of nanocomposites from layered silicates	5
Fig.1.3	Schematic representation of PLS nanocomposite obtained by intercalation of polymer from solution	6
Fig.1.4	Schematic representation of PLS nanocomposite obtained by in situ polymerization	7
Fig.1.5	Schematic representation of nanocomposite obtained direct melt intercalation	8
Fig.1.6	Commercially available E-Glass fibers	10
Fig. 4.1	Mechanical stirrer with oil bath setup	23
Fig. 4.2	Ultrasonication bath	24
Fig. 4.3	Hardener mixing in Epoxy- Nanoclay base	25
Fig. 4.4	Samples before tabbing	25
Fig. 4.5	Actual image of “Tab”	25
Fig. 4.6	Specimen dimensions for flexural test	26
Fig. 4.7	Nanocomposite flexural specimen	26
Fig. 4.8	Specimen dimensions for tensile test without tabs	26
Fig. 4.9	Specimen dimensions for tensile test without tabs	27
Fig. 4.10	Nanocomposite specimen for tensile testing	27
Fig. 4.11	Samples tabbed, clamped & left for drying	27
Fig. 4.12	UTM tensile setup	28
Fig. 4.13	Specimen in jaws	28
Fig. 4.14	UTM flexural setup	29

Fig. 4.15	Specimen positioning	29
Fig. 4.16	Micro hardness tester	29
Fig. 4.17	Schematic representation of x-ray diffraction principle	30
Fig. 4.18	Schematic representation of x-ray diffractometer principle	31
Fig. 4.19	Gold coating equipment	31
Fig. 4.20	SEM machine	31
Fig. 4.21	Schematic of transmission electron microscopy	32
	-	
Fig. 5.1	Indentation in specimen	34
Fig. 5.2	Micro hardness test results	35
Fig. 5.3	X-ray diffractogram of 2 wt% nanoclay	36
Fig. 5.4	X-ray diffractogram of 3 wt% nanoclay	36
Fig. 5.5	SEM images of fracture surface having 2wt% nanoclay	37
Fig. 5.6	SEM images of fracture surface having 3wt% nanoclay	37
Fig. 5.7	TEM Micrograph of 3wt% at 200000X	38
Fig. 5.8	TEM Micrograph of 3wt% at 300000X	38
Fig. 5.9	TEM Micrograph of 3wt% at 400000X	39
Fig 5.10	Flexural Strength vsNanoclaywt % (30° angle)	41
Fig 5.11	Flexural Strength vsNanoclaywt % (45° angle)	42
Fig 5.12	Flexural Strength vsNanoclaywt % (60° angle)	42
Fig. 5.13	Flexural strength of Epoxy/Glass Fiber, 2 wt% Nanoclay/Epoxy/ Glass Fiber and 3 wt% Nanoclay /Epoxy /Glass Fiber at different fiber orientation	43
Fig. 5.14	Tensile Strength vsNanoclaywt % (30° angle)	45
Fig. 5.15	Tensile Strength vsNanoclaywt % (45° angle)	46
Fig. 5.16	Tensile Strength vsNanoclaywt % (60° angle)	46
Fig. 5.17	Tensile strength of Epoxy/F, 2 wt% Nanoclay/Epoxy/ GF and 3 wt% Nanoclay /Epoxy /GF at different fiber orientation	47

## LIST OF TABLES

---

---

<b>Table No.</b>	<b>Title</b>	<b>Page No.</b>
1.1	Important characteristics of Nanocomposites	2
1.2	Comparison of typical properties of some useful glass	10
4.1	Specimen specification for testing	26
5.1	Microhardness values for different clay loading samples	34
5.2	d-spacing of clay epoxy layered silicates	36
5.3	Flexural strength values of different nanoclaywt% specimen at different fiber orientation angles	40
5.4	Mean flexural strength(MPa) and corresponding percentage increase	41
5.5	Tensile strength values of different nanoclaywt% specimen at different fiber orientation angles	44
5.6	Mean flexural strength(MPa) and corresponding percentage increase	45

## **1.1 NANOTECHNOLOGY:**

Nanotechnology is the creation and use of materials or devices at extremely small scale( 1nm =  $10^{-9}$ m.)

Some of the definitions of Nanotechnology are:

The design, characterization, production and application of materials, devices and systems by controlling shape and size at the nanoscale( E. Abad et al. 2005)

The deliberate and controlled manipulation, precision placement, modelling and production of matter at nanoscale in order to create materials, devices and systems with fundamentally new properties and functions.

The US Foresight Institute gives “ Nanotechnology is a group of emerging technologies in which the structure of matter is controlled at the nanometer scale to produce novel materials and devices that has useful and unique properties.”

A very succinct definition of nanotechnology is simply “engineering with atomic precision.”

Nanotechnology is directed towards the formation of various nanomaterials such as: Nanocomposites, Nanofiber, Nanoparticulate fillers etc.

## **1.2 NANOCOMPOSITE:**

A nanocomposite is a multiphase solid material where one of the phases has one, two or three dimensions of less than 100 nanometers (nm), or structures having nano-scale repeat distances between the different phases that make up the material. In mechanical terms, nanocomposites differ from conventional composite materials due to the exceptionally high surface to volume ratio of the reinforcing phase and/or its exceptionally high aspect ratio. The mechanical, electrical, thermal, optical, electrochemical, catalytic properties of the nanocomposite will differ markedly from that of the component materials.

**Table 1.1: Important Characteristics of Nanocomposites**

<b>Improved properties</b>	<b>Disadvantages</b>
Mechanical properties (tensile strength, stiffness, toughness)	Viscosity increase (limits process ability)
Gas barrier	Dispersion difficulties
Synergistic flame retardant additive	Sedimentation
Dimensional stability	
Thermal expansion	
Thermal conductivity	
Chemical resistance	
Reinforcement	

**1.3 CLASSIFICATION OF NANOCOMPOSITES:**

On the basis of matrix, nanocomposites can be classified as:

1. Metal matrix nanocomposites
2. Ceramic matrix nanocomposites
3. Polymer matrix nanocomposites

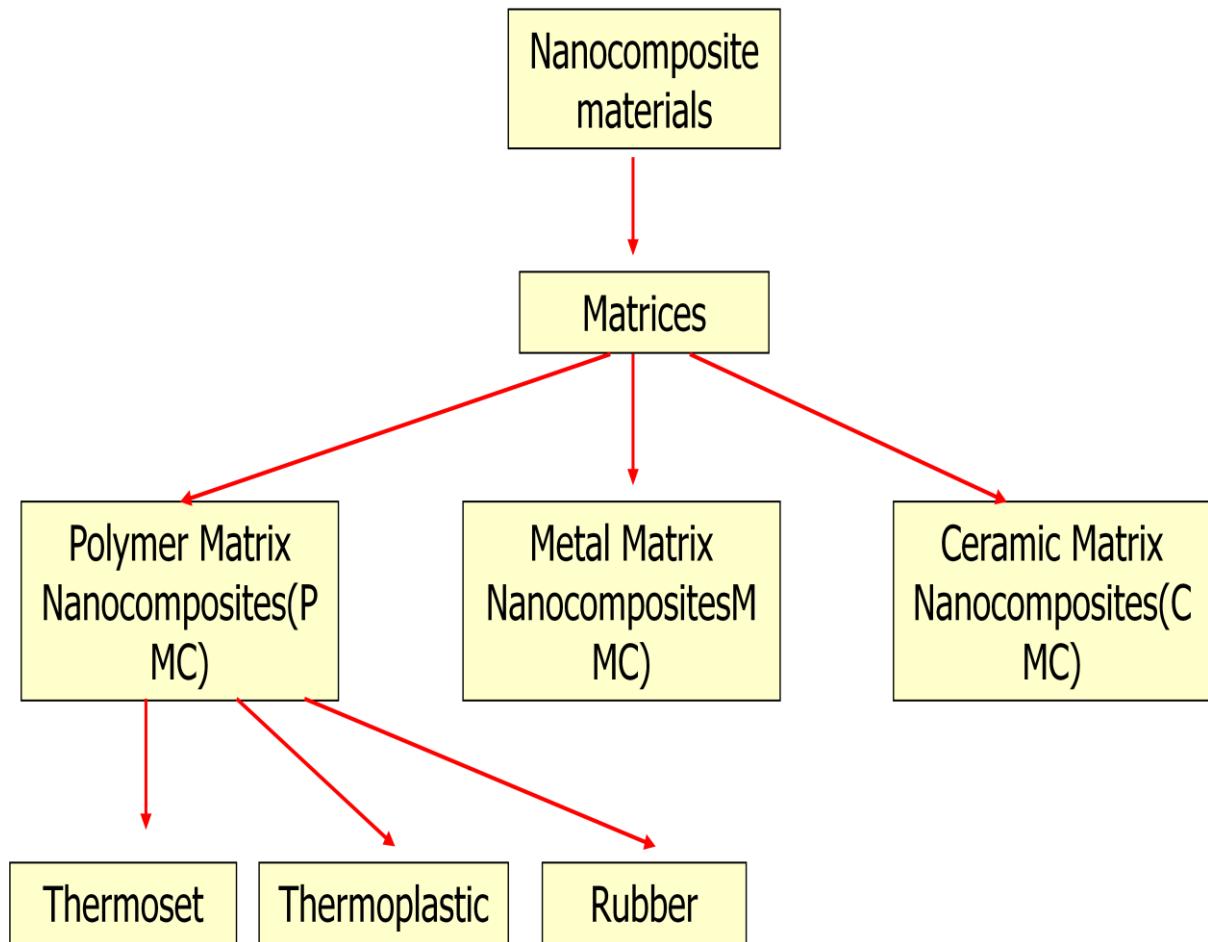


**Fig. 1.1: Classification of Nanocomposites: based on matrices.**

### **1.3.1 Ceramic-matrix nanocomposites:**

In Ceramic-matrix composites the main part of the volume is occupied by a ceramic, i.e. a chemical compound from the group of oxides, nitrides, borides, silicides etc. In most cases, ceramic-matrix nanocomposites encompass a metal as the second component. Ideally both components, the metallic one and the ceramic one, are finely dispersed in each other in order to elicit the particular nanoscopic properties. Nanocomposite from these combinations were demonstrated in improving their optical, electrical and magnetic properties as well as tribological, corrosion-resistance and other protective properties.

### 1.3.2 Metal-matrix nanocomposites:

Metal matrix nanocomposites can also be defined as reinforced metal matrix composites. This kind of composite can be classified as continuous and non-continuous reinforced materials. One of the important nanocomposites is Carbon nanotube metal matrix composites, which are emerging new materials that are being developed to take advantage of the high tensile strength and electrical conductivity of carbon nanotube materials. Critical to the realization of CNT-MMC possessing optimal properties in these areas are the development of synthetic techniques that are (a) economically producible, (b) provide for a homogeneous dispersion of nanotubes in the metallic matrix, and (c) lead to strong interfacial adhesion between the metallic matrix and the carbon nanotubes. In addition to carbon nanotube metal matrix composites, boron nitride reinforced metal matrix composites and carbon nitride metal matrix composites are the new research areas on metal matrix nanocomposites.

### 1.3.3 Polymer-matrix nanocomposites:

In the simplest case, appropriately adding nanoparticles to a polymer matrix can enhance its performance and is particularly effective in yielding high performance composites, when good dispersion of the filler is achieved and the properties of the nanoscale filler are substantially better than those of the matrix. For example, reinforcing a polymer matrix by much stiffer nanoparticles of ceramics, clays, or carbon nanotubes.

Nanoscale dispersion of filler or controlled nanostructures in the composite can introduce new physical properties and novel behaviours that are absent in the unfilled matrices, effectively changing the nature of the original matrix (such composite materials can be better described by the term *genuine nanocomposites* or *hybrids*). Some examples of such new properties are fire resistance or flame retardancy and accelerated biodegradability.

Addition of nanoclay in the polymer results in any one of the following structures depending on the extent of the separation of silicate layers.

1. **Intercalated nanocomposites:** In these Polymer Clay Nanocomposites, the polymer chains are inserted between the layers of the clay such that the interlayer spacing  $d$  is expanded, but the layers still bear a well-defined relationship to each other.

2. **Exfoliated nanocomposites:** In an exfoliated Polymer Clay Nanocomposites, the layers of the clay have been completely separated, and the individual mineral sheets are randomly distributed throughout the polymeric matrix.
3. **Conventional composites (microcomposites):** A third alternative is constituted by the dispersion of whole clay particles within the polymer matrix, but this simply represents the use of clay as conventional filler in the formation of a microcomposite.

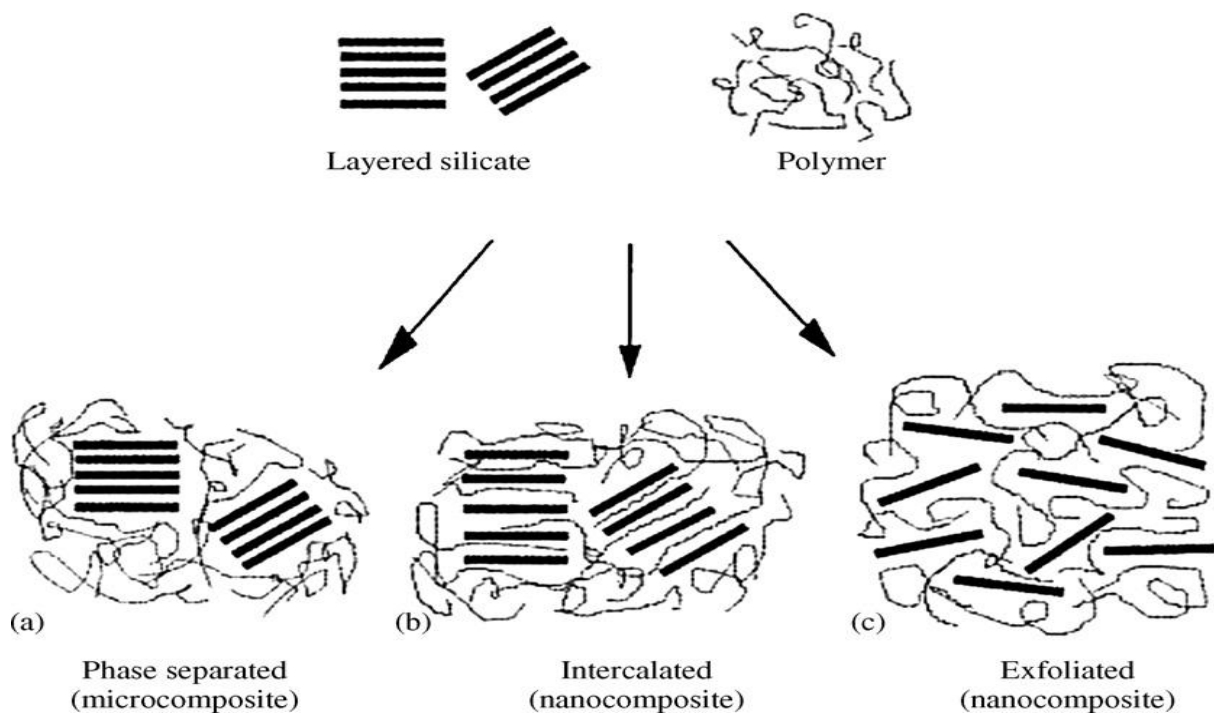


**Fig. 1.2: Schematic representation of basic types of nanocomposites from layered silicates<sup>[1]</sup>**

### **Preparation Methods of Polymer–Clay Nanocomposites:**

The correct selection of the modified clay is essential to ensure the effective penetration of the polymer into the interlayer spacing of the clay and result in the desired exfoliated or intercalated product. Substantially, there are three main methods for preparing Polymer Clay Nanocomposites:

1. **Intercalation of polymer from solution:** This approach is effective at producing organic–inorganic multilayer composites. Owing to the unusual physical chemistry of the intercalation processes involved, it offers the possibility of improving the physical and

mechanical properties of many systems and fabricating electron-conducting materials, e.g., for reversible electrodes. Among the most widespread nanocomposites are polyolefin-MMT, nylon-layered silicates, and epoxy-clay hybrid nanomaterials. This process is based on the choice of a solvent system in which the polymer is soluble and the silicate layers are swellable. The clay is first swollen in a suitable solvent, such as water, chloroform, or toluene. When the polymer and silicate solution are mixed, the polymer chains intercalate and displace the solvent adsorbed within the silicate galleries. Upon solvent removal, the intercalated structure remains, resulting in the corresponding Polymer Clay Nanocomposite. From the application standpoint, however, this method involves the extensive use of solvent. Therefore, exception made for water-soluble polymers, this procedure is usually environmentally unfriendly and economically prohibitive.

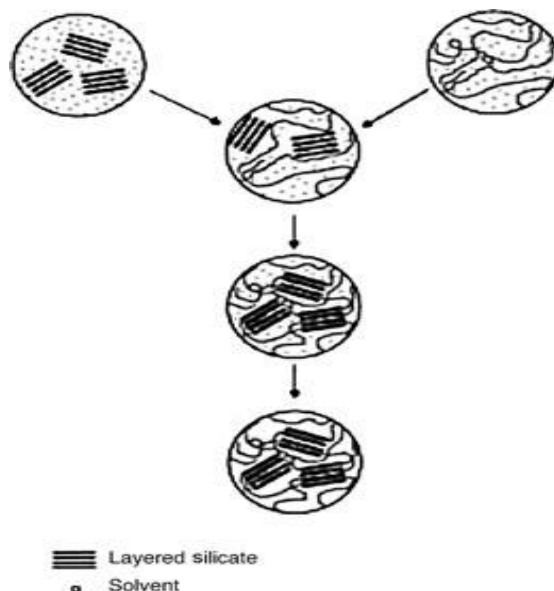


**Fig. 1.3: Schematic representation of PLS nanocomposite obtained by intercalation of polymer from solution<sup>[2]</sup>**

**2. In situ intercalative polymerization method:** The most intriguing type of intracrystalline chemical reaction is the incorporation of monomer molecules into the pores of a host structure, followed by controlled internal transformations into polymer, oligomer, or hybrid-sandwich products (post-intercalative transformations). Monomers intercalated into a clay mineral migrate along its galleries, and, initiated by heat, radiation, or an appropriate agent, polymerization occurs within its layers. This approach is often also called “ship-in-the-bottle” polymerization, and the monomer molecules incorporated through displacement reactions form new hydrogen bonds and other types of intercalation compounds with the host.

The simplest way of intercalating polymers into inorganic structures is by producing hybrid nanocomposites via a one-step emulsion polymerization of conventional monomers in the presence of various organophilic minerals. The physical processes underlying intercalation via emulsion polymerization are as follows. The basis of the swelling characteristic of clays in aqueous systems containing monomer micelles 2–10 nm in size allows the micelles to penetrate into swollen MMT layers. At the same time, the monomer drops forming during solution polymerization are very large (10<sup>2</sup>–10<sup>4</sup> nm) and are simply adsorbed or bound to the surface of MMT particles.

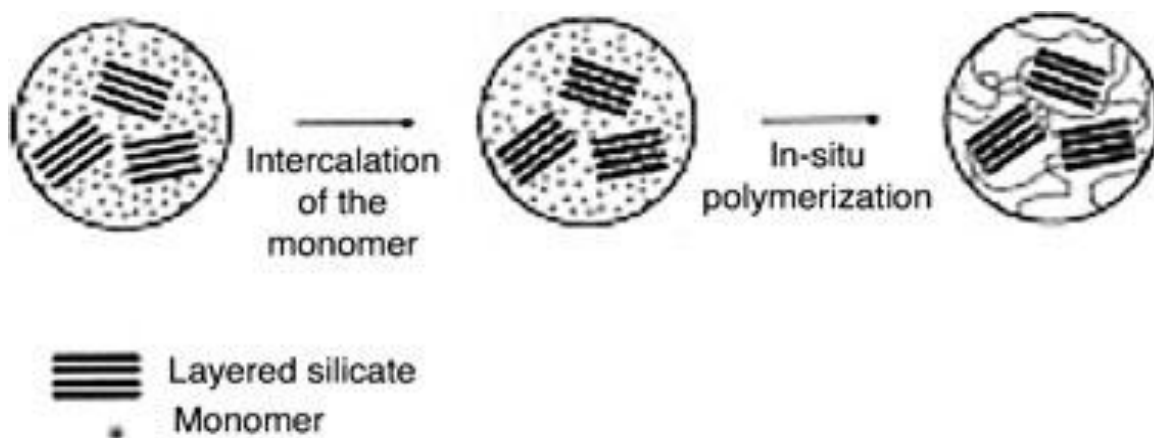


**Fig. 1.4: Schematic representation of PLS nanocomposite obtained by in situ Polymerization<sup>[2]</sup>**

**3. Melt intercalation method:** This technique involves annealing a mixture of the polymer and organoclay above the polymer softening point. While annealing, the polymer chains diffuse from the bulk polymer melt into the galleries between the silicate layers. A range of nanocomposites with structures from intercalated to exfoliated can be obtained, depending on the degree of the penetration of the macromolecular chains in the interlayer spaces. Outcome of polymer intercalation depends critically on silicate functionalization and constituent interactions. An optimal starting interlayer structure balance of polar/hydrophobic interactions between the polymer chains and the organoclay are two key issues for a successful melt intercalation process. Contrary to process (a), in which entropy is claimed to be the driving force leading to PCN formation, in melt intercalation the enthalpic component ( $\Delta H$ ) of the Gibbs free energy ( $\Delta G$ ) seems to govern the system thermodynamics (Vaia and Giannelis,

1997b). In fact, in this case the entropy loss associated to the confinement of the polymer melt within the silicate galleries is compensated by the entropy gain of the aliphatic chains of alkylammonium cations associated to the concomitant layer separation, resulting in an entropy change  $\Delta S \approx 0$ . The favorable enthalpy is due to the increase in favorable interaction energy between the polymer and the organoclay, due to the formation of weak, hydrogen-like bonds, dipole–dipole, and vander Waals interactions. Overall, this method has great advantages over both processes (a) and (b). In fact, (1) it is environmentally benign as no solvent is employed, and (2) it is totally compatible with current polymer industrial processes such as extrusion or injection molding. Accordingly, the melt intercalation technique has become the standard for the preparation of PCNs

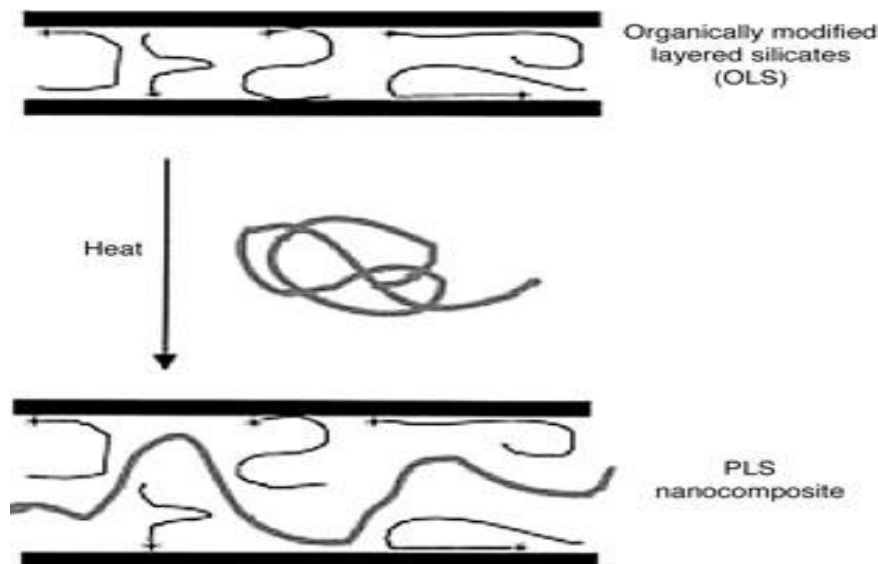


**Fig. 1.5: Schematic representation of nanocomposite obtained direct melt intercalation<sup>[2]</sup>**

#### **Properties of Polymer–Clay Nanocomposites:**

Nanomaterials additives can provide many property advantages in comparison to both their conventional filler counterparts and base polymers. Properties that have been shown to undergo substantial improvements include:

- Mechanical properties (e.g., strength, modulus, and dimensional stability)
- Decreased permeability to gases, water, and hydrocarbons
- Thermal stability and heat distortion temperature
- Flame retardancy and reduced smoke emissions

- Electrical conductivity
- Chemical resistance
- Optical clarity in comparison to conventionally filled polymers

In addition, it is important to recognize that nanoparticulate/ fibrous loading significantly improves property with very low loading levels, traditional nanoparticle additives requiring much higher loadings to achieve similar performance. This, in turn, can result in substantial weight reductions (of obvious importance for various military and aerospace applications) for similar performances, greater strength for similar structural dimensions, and, for barrier applications, increased barrier performance for similar material thickness

#### **1.4 GLASS FIBER**

Glass fibers are among the most versatile industrial materials known today. They are readily produced from raw materials, which are available in virtually unlimited supply. All glass fibers described in this article are derived from compositions containing silica. They exhibit useful bulk properties such as hardness, transparency, resistance to chemical attack, stability, and inertness, as well as desirable fiber properties such as strength, flexibility, and stiffness. Glass fibers are used in the manufacture of structural composites, printed circuit boards and a wide range of special-purpose products.

#### **Glass fibre is available in the following forms:**

- A. Continuous Fibre
- B. Chopped strands
- C. Woven Fabric.

#### **The types of glass fiber:**

1. **E-glass (electrical)** - lower alkali content and stronger than A glass (alkali). Good tensile and compressive strength and stiffness, good electrical insulation, relatively low density, non-flammable, good chemical resistance, relatively insensitive to moisture and relatively low cost, but relatively low fatigue resistance and impact resistance. E-glass is the most common form of reinforcing fibre used in polymer matrix composites.

**Composition of E-glass:** SiO<sub>2</sub> 54wt%, Al<sub>2</sub>O<sub>3</sub> 14wt%, CaO+MgO 22wt%, B<sub>2</sub>O<sub>3</sub> 10wt% and Na<sub>2</sub>O+K<sub>2</sub>O less than 2wt%. Some other materials may also be present at impurity levels.



**Fig. 1.6: Commercially available E-Glass fibers**

2. **C-glass (chemical)** - best resistance to chemical attack. Mainly used in the form of surface tissue in the outer layer of laminates used in chemical and water pipes and tanks.
3. **R, S or T-glass** – manufacturers’ trade names for equivalent fibres having higher tensile strength and modulus than E glass, with better wet strength retention. Higher Inter Lamina Shear Strength and wet out properties are achieved through smaller filament diameter. Developed for aerospace and defense industries, and used in some hard ballistic armour applications. This factor, and low production volumes mean relatively high price.
4. **A-glass**- Soda lime glass with high alkali content between 10-15%. Very poor mechanical properties but high resistant to chemical attacks.
5. **D-Glass**- Improved dielectric glass developed for high performance electronic applications.

**Table-1.2 Comparison of typical properties of some useful glass**

Materials	Density (g/cm <sup>3</sup> )	Tensile Strength (MPa)	Young modulus (GPa)
E-Glass	2.55	2000	80
S-Glass	2.49	4750	89
Alumina (Saffil)	3.28	1950	297
Carbon	2.00	2900	525
Kevlar 29	1.44	2860	64
Kevlar 49	1.44	3750	136

## **E- glass Applications:**

The use of E-Glass as the reinforcement material in polymer matrix composites is extremely common. Optimal strength properties are gained when straight, continuous fibres are aligned parallel in a single direction. To promote strength in other directions, laminate structures can be constructed, with continuous fibres aligned in other directions. Such structures are used in storage tanks and the like. Random direction matts and woven fabrics are also commonly used for the production of composite panels, surfboards and other similar devices.

## **1.5 EPOXY RESIN**

Epoxy resin systems have achieved acceptance as adhesives, potting compounds, molding compounds and as matrices for continuous filament composites used in structural applications. Here, we discuss epoxy resins in their role as matrices in fiber composites. In this role, they possess several advantages over other types of polymers. The main advantages are:

- inherently polar nature that confers excellent adhesion to a wide variety of fibers.
- relatively low cure shrinkage that makes dimensional accuracy of fabricated structures easier to obtain.
- no volatile by-products of the curing reaction to cause undesired bubble or void formation.
- crosslinked structure that confers excellent resistance to hostile environments, both aqueous and nonaqueous

In addition to these advantages, epoxy resins have tremendous versatility because they can be formulated to meet a broad range of specific processing and performance requirements.

## **1.6 FIBER REINFORCED EPOXY/CLAY NANOCOMPOSITE**

Fiber reinforced epoxy/clay nanocomposites are those in which epoxy modified with nanoclay is used with fibers. The dispersion of nanoclay in epoxy is achieved by mechanical stirring followed by ultrasonication. The fiber reinforced nanocomposites are then prepared by any of the conventional composites manufacturing technique ( hand layup, vacuum bagging, vacuum assisted resin transfer moulding etc). The resulting nanocomposite exhibit better mechanical properties, barrier properties and fire retardancy.

**EmrahBozkurt et al.(2007)** investigated the mechanical and thermal properties of non-crimp glass fiber reinforced clay/epoxy nanocomposites. E-glass non-crimp fabrics, epoxy thermosetting resin and Na<sup>+</sup>montmorillonite (MMT and OMMT) clay particles were used to fabricate specimen. The clay/epoxy mixture was mechanically stirred for about 1hour at room temperature followed by ultrasonication for 20min in order to further exfoliate the clay within the resin. Hand Layup technique was used to impregnate and laminate the composite structures. Clay/epoxy nanocomposites were synthesized with different concentrations of MMT and OMMT clay. X-ray analysis of surface treated and untreated clays reveal that the modification of clay increased the d-spacing of clay layers that ease the dispersion of clay particles in the matrix. The tensile strength and modulus values remains almost constant by the addition of MMT and OMMT up to 6 wt% clay contents as compared to those fabricated without clay addition. However, further addition of MMT and OMMT reduced the strength values. On the other hand, tensile modulus values are reduced by the addition of OMMT while they remained constant with MMT addition at 10 wt% clay loading. Flexural strength and modulus values are increased with the addition of MMT and OMMT, up to 6 wt% of clay loading. Maximum improvement in flexural strength and modulus is obtained at 6 wt% clay content and by the addition of nanoparticulates the flexural strength and modulus are improved by 16% and 13%, respectively. With the addition of OMMT (10 wt%) particles to the matrix, fracture toughness of laminates increased by 5%. Addition of clay significantly reduces the flammability of polymer composite. The average extends of burning and average time of burning is reduced by 55% and 77%, respectively due to the addition of 10 wt% MMT into epoxy. This improvement was even higher with surface treated clay (OMMT) due to its better dispersion in the polymer matrix.

**BetimeNuhiji et al.(2011)** investigated the effect of both the mixing technique and heating rate during cure on the dispersion of montmorillonite(MMT) clay in an epoxy resin. A two part epoxy thermoset ‘EPON 828’ based on diglycidyl ether of bisphenol A/epichlorohydrin(DGBEA) and ‘Ardur 2954’ alongwith I.30E MMT clay was used to synthesize the specimen. MMT clay corresponding to 5 wt% of epoxy resin was combined with a given amount of ‘EPON 828’ resin and heated to 70°C. This mixture was stirred for 2h

using a magnetic stirrer. The sonication technique was utilised for 30 min to facilitate the dispersion of clay. Epoxy/clay nanocomposites were heated to 130°C at either 3°C ± 1°C/min or 10°C ± 2°C/min and held isothermally for 30 min. Vacuum had been maintained at -70 KPa during cure to prevent the mixture from boiling. The increase in heating rate from 3°C/min to 10°C/min during cure reduced the viscosity by 60% facilitating the penetration of polymer chains into clay galleries. With high amplitude sonication dispersion technique combined with rapid heating rate resulted in two fold increase in clay gallery distances. As the degree of dispersion was enhanced, the flexural modulus and strength properties were found to increase by 15% and 40% respectively.

**Nor Hamidah Mohd. Zulfi & Chow Wen Shyang (2010)** studied the flexural and morphological properties of Epoxy/GF/Silane treated Organo- Montmorillonite Composites. The diglycidyl ether bisphenol A (DGEBA) E glass, a cycloaliphatic amine hardener HY2964 and nanomer 1.30E OMMT were used to fabricate the specimen. The ratio between DGEBA and hardener was 10:6 by weight. 3wt% of OMMT was added to the DGEBA resin. The mixture was stirred at 100rpm upto 10 minute and then hardener is added and further stirred upto 10 min. Four plies of chopped strands mat were used and hand layup method was used to fabricate the specimen. Samples were cured in an oven at 100°C for 60 minute. The incorporation of silane-treated OMMT increases the stiffness of the E/GF composites significantly. The flexural modulus of E/GF/OMMT is 4.41 GPa. Note that the flexural modulus increased significantly as the loading of silane-treated OMMT increased. In addition the flexural modulus of E/GF/Si-15/OMMT is approximately 4.98 GPa, which is an increase of 13%. This result is due to the exfoliation of silicate layers in the E matrix. The improvement in modulus could also be attributed to the high aspect ratio, contact surface and reinforcing effects of the silane-treated OMMT.

**Mo- Lin Chan et al. (2011)** studied the basic reinforcing mechanism of the composites, particularly the interaction between nanoclay and surrounding matrix. Uniformly-dispersed nanoclay/ epoxy composite samples, based on tailor-made experiment setup were fabricated. Araldite GY251 epoxy resin and hardener HY956 in the ratio of 5:1 were used to produce nanoclay/epoxy composites. During the process of fabricating the composites, the organomodified nanoclay (SiO) was added into the resin in predetermined weight content. The nanoclay/epoxy resin was placed on a rotating platform and put into a bell jar under vacuum for 55 min to extract gas bubbles. Angular acceleration and deceleration motions

were applied through the rotation of the platform from 0 to 930 rpm for 2 s and then returned back to 0 rpm for 1 s. The mixture was then rest for another 7s. In order to ensure that the nanoclay inside the mixture was uniformly-dispersed, repeated motions by following the previous steps were applied for 5 min. The hardener was then added to the mixture. Spinning of a new mixture was then applied again by using aforementioned procedure for 1 h under vacuum condition till the viscosity increased to avoid any movement of the nanoclay inside the resin. All samples were then removed from the jar. All composites with the nanoclay content of 1 wt.%, 3 wt.%, 4 wt.% 5 wt.% and 7 wt.% and four identical samples for each type of composites were made. The increase of the tensile strength of the samples with 3 wt.%, 4 wt.% and 5 wt.% of nanoclay are 12%, 16% and 25% respectively. Young modulus of the samples with 5wt% of nanoclay was increased by 28%. The stiffness of the samples with 3 wt.%, 4 wt.% and 5 wt.% of nanoclay increased by 24%, 31% and 34% respectively. Images obtained from scanning electron microscopy (SEM) and results extracted from transmission electron microscope (TEM) proved that interlocking and bridging effects did exist in the composites. Nanoclay clusters with the diameter of 10 nm could enhance the mechanical interlocking inside the composites and thus, breaking up the crack propagation. The formation of boundaries between the nanoclay clusters and epoxy can refine the matrix grains and further improve the flexural strength of the composites.

**Jong *et al.* (2002)** investigated the mechanism of nanoclay exfoliation in epoxy clay nano composites system. The elastic force exerted by cross-linked epoxy molecules inside the clay galleries was found responsible for exfoliation of clay layers from the intercalated tactoids. Complete exfoliation of clay galleries was observed under the conditions of slow increase of complex viscosity and fast rise of storage modulus. It was observed that faster intra gallery polymerization, though expedited the exfoliation process, was not necessary for exfoliation. It was also observed that clays containing hydroxylated quaternary ammonium ions and quaternary ammonium ions with no polar functional groups produced exfoliated structures equally easily, provided the ratio of storage modulus to complex viscosity was maintained. Both higher curing temperature and the presence of organically modified clay particles accelerated the formation of gels, and the gel time presented an upper bound of time available for exfoliation.

**Jinwei Wang, Shuchao Qin(2007)** investigated the effect of ultrasonic stirring time on the mechanical and thermal properties of epoxy–nanoclay composites. The bisphenol A diglycidyl ether (D.E.R.332) was added in a 500 ml beaker that was heated to 80 °C, followed by the addition of curing agent 4,4'- diaminodiphenylsulphone under mechanical stirring at 400 rpm for about 30 min until the curing agent dissolved. The organophilic clay (I.30E) 5.0 wt% of the epoxy resin was then added to the beaker under continuous mechanical stirring at 400 rpm at 80 °C for 2 h. The mixture was transferred to a capped bottle which was then immersed in an ultrasonic bath for ultrasonic stirring. The diffusion of the epoxy and curing agent into the clay layer, and the curing reaction of epoxy with amine could be promoted by the ultrasonic stirring. With the increase in ultrasonic stirring time, the clay layer could be separated further; the curing reaction was promoted, and the cross linking system with branched alkyl chain was obtained. The thermal decomposition temperature of the composite could be improved by the elongation of the stirring time. However, both the glass transition temperature and the storage moduli of the composites decreased with increase in ultrasonic stirring time.

**L. Aktas and M. C. Altan(2010)**, investigated the effect of nanoclay content on the properties of glass fibre reinforced, waterborne epoxy laminates. Fourteen ply nanocomposite laminates containing 0, 0.1, 0.2, 0.5, 1 and 2 wt% cloisite Na<sup>+</sup> nanoclay were fabricated by a hot press. The interlaminar shear strength, flexural strength and flexural stiffness of the fabricated nanocomposites were characterised. In addition, the thermal stability of the laminates was investigated using thermogravimetric analysis, the state of dispersion was studied by X-ray diffraction, and the fibre–matrix adhesion was assessed using scanning electron microscopy on fracture surfaces. Mechanical properties peaked at a nanoclay loading of 0.5 wt%. At this low nanoclay loading, the improvements in interlaminar shear strength, flexural strength and flexural stiffness were 5, 8 and 12% respectively. Thermogravimetric analysis indicated moderate improvements in thermal stability. X-ray diffraction, on the other hand, indicated complete exfoliation of nanoclay platelets for 0.1, 0.2 and 0.5 wt% loadings. A subtle peak appeared for nanoclay loadings of 1 and 2 wt% at gallery spacing of 17 Å. Scanning electron micrographs indicated improved fibre–matrix adhesion with increasing nanoclay content as evidenced by increased amount of matrix residues on the fibre bundles after fracture.

**Mahmood M Shokrieh et al.(2011)** investigated the effect of time exposure at low temperatures on the mechanical response of quasi-isotropic composites. E-Glass fiber-reinforced epoxy was used to prepare laminates with quasi-isotropic stack sequence. Hand lay-up method was used to fabricate thin laminate composed of fifty plies of reinforcement with epoxy resin 'ML-506' with hardener HA11, giving a laminate approximately 10 mm in thickness. Charpy test specimens were cut from laminates with 10 mm width. The V-notch of 45° in two different directions and with different span length-to-depth ratios is prepared by a milling machine. Impact energy decreases with the decrease of the test temperature. On the other hand, specimens after 10 days exposure to low temperature show slightly lower impact energy absorption than the specimens with one day exposure at considered temperatures. At each temperature, with increasing energy level, the crack length and delamination length were increased. A higher delamination on specimens was found with increasing the testing temperature. While less crack length occurred, when the specimen temperature increased. Results show that the impact strength decreased by increasing the specimens span length to depth ratio above 6. This phenomenon was found for both case of one and ten days exposure to low temperature. Two different failure processes were observed for specimens with side-on and edge-on notch orientations. The specimen with side-on notch orientation partly delaminates by failure of the weak interface planes of matrix materials between the plies of laminate due to shear stresses. However, for edge-on notch orientations, failure concentrates on the glass reinforcements, glass fiber breakage under the influence of tensile stresses ahead of the notch represents the dominating failure process. By visual inspection, it is found that failure mechanism changes from matrix cracking at room temperature to delamination and fiber breakage at low temperatures. Microscopic examination shows that for sideon notch orientation, by increasing test temperature, more delamination and matrix cracking were observed. In addition, more fiber breakage was found in the case of edge-on notch orientation by increasing the test temperature. Results of the current research indicated that in spite of significant increase in mechanical properties of composites at low temperatures under static loading, but impact response of composites reduced by decreasing temperature. This can be explained such that mechanical properties of composites are different under static and dynamic loading at low temperatures. This is because the material constituents become more brittle as temperature decreases and are less able to blunt cracks and consequently composite absorbed less energy during impact test.

**Marino Quaresimin et al.(2012)** assess the benefits derived from the matrix nanomodification of composite laminates. Fracture toughness and crack propagation resistance for neat and clay modified epoxy, interlaminar shear strength, delamination resistance for base and clay modified epoxy laminates has been studied. Due to a very low viscosity and long average life at 25°C, A DGEBA based epoxy resin which is especially suited for resin infusion technique was used along with an amminichardner in the ratio 3:1 for each investigated nanofiller content. Surface modified lamellae of montmorillonite 1nm thick and with lateral dimensions from 70 to 150nm, namely Cloisite 30B and RXG 7000 were used for nanomodification. Twill glass fibre VV-350T had been used as reinforcement for neat and nanomodified epoxy laminates. The nanoclays were dispersed in the resin through a shear mixing process at about 3500 rpm for 1 hour in order to get an as good as possible distribution and dispersion of the nanofiller within the resin, promoting nanoclays intercalation/exfoliation and breaking of nanoclay clusters. Sonication process was carried out for about 40 min to reach the finer results. Then hardener was added and shear mixing of the overall system was done for further 10 min just to improve the resin hardener mixing.

Tensile strength of the epoxy clays slightly decreased with the increase of clay content. Improvement of elastic modulus of the modified resin with respect to neat epoxy. 3wt% cloisite 30B laminates exhibit a slightly improved interlaminar shear strength while RXG 7000 laminates does not exhibit significant improvement. Cloisite 30B nanomodified resin exhibits the highest fracture toughness, about a 40% higher than that of the neat resin. For higher nanofiller content, the 30B nanomodified resin is monotonically decreasing, while RXG7000 toughness increases again after 3 wt.%. It was observed that clay loading results in an improved crack propagation resistance.

**Zainuddin et al. (2010)** analysed the effect of environmental conditioning especially under hot-wet conditions on E-glass epoxy fiber reinforced composite. The weight gain was higher for all the wet conditions samples exposed to elevated temperatures. Addition of 1–2 wt% of nanoclay decreased the weight gain. Flexural properties were found to degrade with increase in time. 2 wt% GFRP composites showed enhancement in properties under all conditions over neat counterparts. In some cases, samples subjected to hot dry condition at 60<sup>0</sup>C showed increase in properties over room temperature conditioned samples. Scanning electron micrographs provided clear evidence of the effects of nanoclay, elevated temperature and moisture absorption. Enhancement in interfacial bonding was observed in 2wt.% composite samples, both at room temperature and hot-wet conditioning.

**Li-Yu-Lin et al. (2006)** studies the Preparation and characterization of layered silicate/glassfiber/epoxy hybrid nanocomposites via vacuum-assisted resin transfer moulding (VARTM). Unidirectional glass fibers were placed in two directions: parallel and perpendicular to the resin flow direction. The intercalation behaviour of the clay and the morphology of the composites were investigated using X-ray diffraction (XRD) and transmission electron microscopy (TEM). The complementary use of XRD and TEM techniques revealed an intercalated clay structure in the composites. Dispersion of clay in the composites was also observed using scanning electron microscopy (SEM); the observed clays were dispersed between both the bundles of glass fibers and within the interstices of the fiber filaments. The mechanical properties of the ternary composites were evaluated. The results indicated that introducing a small amount of organoclay to the glass fiber/epoxy composites enhanced their mechanical and thermal properties, confirming the synergistic effects of glass fibers and clays in the composites.

**Isiket al. (2003)** synthesized Diglycidyl ether of bisphenol A type epoxy resin-polyether polyol organically treated montmorillonite ternary nanocomposites. The effects of addition of polyether polyol as an impact modifier on morphological, thermal and mechanical properties of nanocomposites were investigated by X-ray diffraction, scanning electron microscopy (SEM), differential scanning calorimetry, impact and tensile testing. The results showed that organically treated montmorillonite is intercalated by epoxy, since the interlayer spacing expanded from 1.83 to 3.82 nm upon nanocomposite synthesis. The addition of polyether polyol impact modifier had no effect on the interlayer spacing. SEM examination showed that polyol forms an immiscible phase in the epoxy matrix. In polyether polyol modified nanocomposites, the impact and tensile strengths decreased with respect to increasing amount of montmorillonite and showed a maximum with respect to the polyether polyol content at constant clay loading.

**Sinha Ray et al. (2003)** studied the academic and industrial aspects of the preparation, characterization, materials properties, crystallization behaviour, melt rheology and processing of polymer/layered silicate nanocomposites. Smectite are a valuable mineral class for industrial applications because of their high cation exchange capacities, surface area, surface reactivity, adsorptive properties. Hectorite and montmorillonite are among the most commonly used smectite-type layered silicates for the preparation of nanocomposites. They

suggested that these composites are generally exhibit improved mechanical properties compared to conventional composites. They exhibit a remarkable increase in thermal stability, as well as self-extinguishing characteristics for flammability, such that the flammability of pristine polymers are significantly reduced after nanocomposite formation with layered silicate.

**Salahuddin et al. (2002)** prepared a highly filled epoxy-montmorillonite (MMT) nano composite using an organically modified MMT. Composites with clay content up to 70 wt. % exhibit unusual transparencies, which is related to the spatial distribution of the mineral nano domains. Dispersion of the layered silicate within the cross linked epoxy matrix was verified using X-ray diffraction pattern, revealing layer spacing of 30 and 70 d-spacing. Examination of these materials by scanning electron microscopy and transmission electron microscopy showed that intercalates have wholly layered morphology at all scales, oriented parallel to the surface of the specimen and have good wetting to the silicate surface by the epoxy matrix. Silicate lamellae intercalated with epoxy resin assembled into a cluster of about 50–120 nm thickness. These clusters assembled into super clusters with an average thickness of 300 nm. Studies by the Vickers hardness test of an epoxy-MMT nano composite containing 60 wt. % MMT indicated that the diamond pyramid hardness was 10–29 kg/mm<sup>2</sup>.

**Manjunatha et al. (2009)** investigated the tensile fatigue behaviour of a silica nanoparticle-modified glass fiber reinforced epoxy composite. The epoxy resin was a standard diglycidyl of Bisphenol A with an epoxide. The GFRP composite laminates were manufactured by resin infusion under flexible tooling technique. An anhydride-cured thermosetting epoxy polymer was modified by incorporating 10 wt. % of well-dispersed silica nanoparticles. The fatigue life of 10 wt. % silica nanoparticle-modified bulk epoxy was about three to four times higher than that of neat epoxy. The fatigue life of the GFRP composite with 10 wt.% silica nanoparticle modified epoxy matrix was about three to four times higher than that of the GFRP with the neat epoxy matrix. The suppressed matrix cracking and reduced crack growth rate due to the particle debonding and plastic void growth mechanisms appeared to contribute for the observed enhancement of the fatigue life in the GFRP with the nanoparticle-modified matrix.

**W. S. Chow(2007)** studies Water absorption of epoxy/glass fiber/organo-montmorillonite nanocomposites. The epoxy/glass fiber/organo-montmorillonite (OMMT) nanocomposites were prepared by hand lay up method. In the previous work, the flexural and morphological properties of the epoxy/glass fiber/OMMT were studied. In this work, the epoxy nanocomposites were characterized by X-ray diffraction (XRD), differential scanning calorimetry (DSC) and water absorption tests. The exfoliation of OMMT in epoxy/glass fiber nanocomposites was detected by XRD. DSC results showed that the glass transition temperature (T<sub>g</sub>) of epoxy was increased slightly in the presence of OMMT. Water uptake of epoxy was reduced by the addition of glass fiber and OMMT. The decrease of water absorption in epoxy is attributed to the increasing of tortuosity path for water penetration in the epoxy composites by the hybrid of glass fiber and OMMT.

**Witchuda Daud et al.(2009)** studies Layered silicates nanocomposite matrix for improved fiber reinforced composites properties. Three-phase glass fiber reinforced composites (GFRP) consisting of traditional woven glass fiber and polyamide-6 (PA6) matrix dispersed with organically modified layered silicates were prepared and investigated in this study. The fabrication of GFRP with different weight percentages of layered silicates was successful when the matrix contains less than 5 wt% of the layered silicates. The improvement due to the high aspect ratio and high stiffness of the layered silicates was illustrated through the matrix-controlled properties of the GFRP. The results showed that the GFRP with 5 wt% layered silicates offer the largest improvement of approximately 30% increase in both flexural strength and compressive strength at elevated temperatures. On the other hand, the in-plane shear properties of laminates revealed that the layered silicates help improved both the in-plane shear strength and modulus appropriately. By utilizing a nanocomposite matrix, improvement of stiffness and strength, as well as thermal and barrier properties is obtained without any change in processing temperature of the fiber composites.

### 3.1 GAPS IN LITERATURE

From the literature studied so far, an important gap found is that the effect of varying nanoclay content and with different fiber orientation on properties of fiber reinforced nanocomposites has not been studied. Efforts are done in the present work to fulfill the gap.

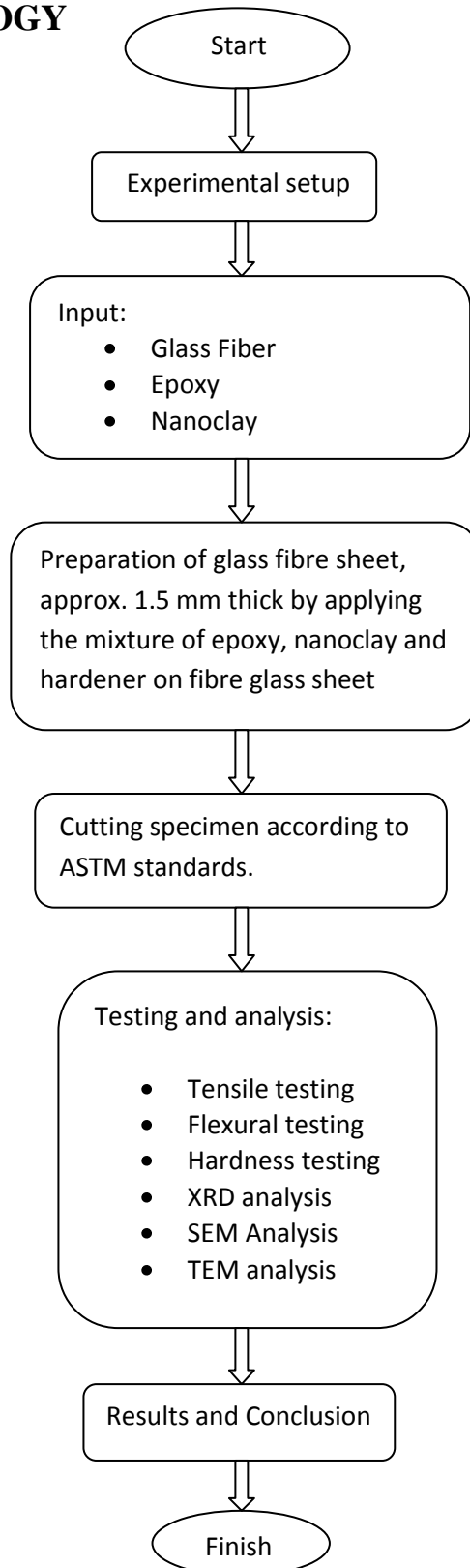
### 3.2 RESEARCH PROBLEM

The present study is mainly focused upon the synthesis and characterization of fiber reinforced epoxy composites. In this study the effect of varying nanoclay concentration and fiber orientation on mechanical properties of nanocomposites has been studied.

### 3.3 OBJECTIVES

1. To synthesize and characterize fiber reinforced epoxy nanocomposites.
2. To study the effect of nanoclay content on tensile and flexural properties of laminas with different fiber orientations.

4.1 METHODOLOGY



## 4.2. FABRICATION OF SPECIMEN

### 4.2.1. MATERIAL

Unidirectional **E-glass fibre** and **M BraceSaturant<sup>®</sup>**, a two part epoxy resin( Density- 983kg/m<sup>3</sup>) was purchased from **BASF Construction Chemicals (India) Private Limited**. Organically modified nanoclay**Closite 30B<sup>®</sup>** was purchased from **Connell Bros. Mumbai**.

### 4.2.2. PROCESSING

#### 4.2.2.1. Cutting Glass Fiber Sheet

For the experimentation unidirectional roll of glass fibre was purchased having 150mm width having 45<sup>0</sup> fibre orientation woven with polymer fibres. The sheets were initially cut from roll in lengths of 600 mm.

#### 4.2.2.2. Mixing of Nanoclay into Epoxy (base):

##### **Mechanical stirring:**

Epoxy base is a thick fluid having blue colour. Mixing of nanoclay in the epoxy base is quite difficult manually. So mechanical stirrer at 2000 rpm alongwith an oil bath was used for proper mixing of nanoclay (Fig. 4.1). Purpose of Oil bath was to heat up the epoxy to desired (80°C) temperature, so that the viscosity of epoxy base can be reduced. Proper mechanical stirring of epoxy base in this manner resulted in better dispersion of clay.



**Fig. 4.1: Mechanical stirrer with oil bath set-up**

Different weight percentages i.e. 2% & 3% by weight of epoxy, of organically modified nanoclay which is preheated at 55<sup>0</sup> C were added and stirred at a temperature of 80°C for 1 hours.

#### **Ultrasonication after Mechanical Stirring:**

Sonication is an act of applying soundenergy to agitate particles in a sample, for various purposes. In the laboratory, it is usually carried out using an ultrasonic bath or an ultrasonic probe, colloquially known as a sonicator. Sonication can be used to speed dissolution, by breaking intermolecular interactions. Sonication was done for evenly dispersing nanoparticles in liquids. After mechanical stirring of the epoxy solution container was placed into the ultrasonication bath for up to 3 hours at 55°C.



**Fig.4.2: Ultrasonication bath**

#### **4.2.2.3. Mixing of Epoxy Base Solution with Hardener:**

After ultrasonication, the solution was mixed with the hardener in the ratio 10:4 by volume. Mixing was done in mechanical stirrer up to 5 to 10 minutes. Mechanical stirrer was used for better mixing of hardener in the resin. The procedure is as shown in figure 4.3.



**Fig. 4.3: Hardener mixing in Epoxy-Nanoclay base**

#### **4.2.2.4. Coating of Nanoclay mixed Epoxy to Glass Fiber Sheets:**

The mixture was then poured on to the glass fiber mat and applied uniformly using the handlayup method. For this, steel scraper was used to maintain uniformity of the solution. It was made sure that there was no air bubbles entrapped inside the epoxy applied on sheet otherwise it would create a flaw there. After applying epoxy, the sheet took overnight to dry and then epoxy coating was done on other side following same procedure. The full curing of sheet was done by leaving it under ambient temperature for at least seven days before processing further.

#### **4.2.2.5. Sizing of Sheet for Samples and Tabs**

Once the epoxy was fully cured, the sheet was cut to actual sample size using the cutting machine. The tabs were also cut with same cutting machine (Fig. 4.4 & Fig. 4.5).



**Fig. 4.4 Samples before tabbing**



**Fig.4.5: Actual image of “Tab”**

### Specimen Specifications

The specimens had been cut and prepared as per the ASTM standards D3037/3039 and D790 for tensile and bending tests respectively. The dimensions of specimens are shown below.

**Table 4.1 Specimen specification for testing**

Parameters for specimen	Specimen for tensile testing	Specimen for flexural testing
Length	250mm	125mm
Width	15mm	12.7mm
Thickness	1.5mm	1.5mm
Tab length	56mm	-
Tab thickness	1.5mm	-

### Specimen Dimensions

- For flexural test

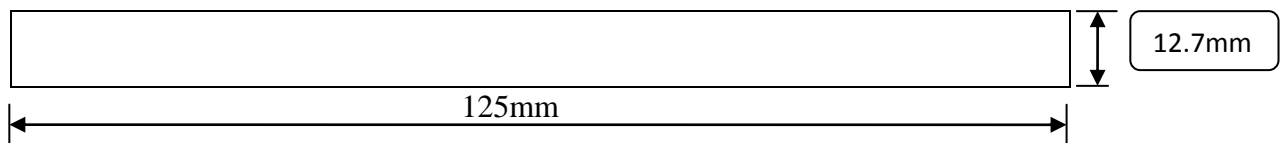


**Fig.4.6: Specimen dimensions for flexural test**



**Fig.4.7: Nanocomposite flexural specimen**

- For tensile test

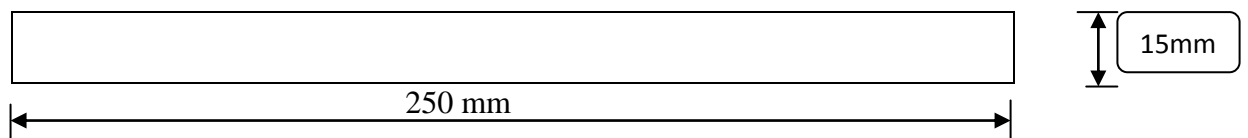


**Fig.4.8: Specimen dimensions for tensile test without tabs**

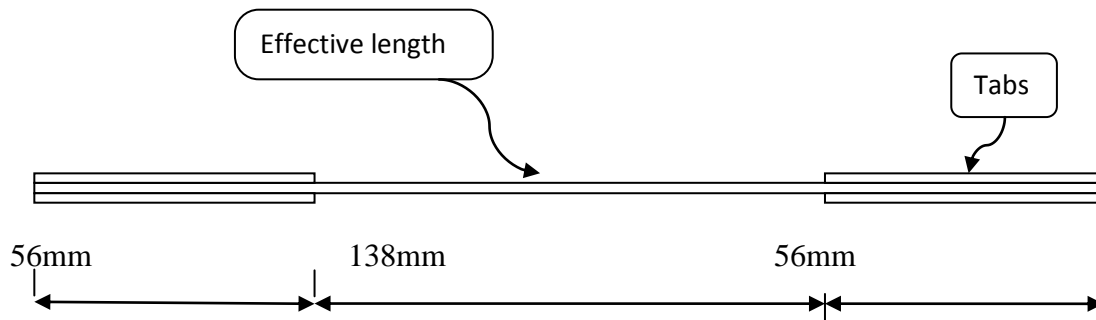


**Fig.4.9: Specimen dimensions for tensile test with tabs**



**Fig.4.10: Nanocomposite specimen for tensile testing**

#### 4.2.2.6. Placing Tabs on Samples

The samples had to be tabbed on both side on two ends. We prepared the mixture of araldite and carefully apply it on the both side of sample. The tabs were now placed on both side of araldite pasted sample. The araldite would act as binder between tab and actual sample.



**Fig. 4.11: Sample tabbed, Clamped and left for drying**

Two paper clamps were placed on both tabbed side to hold tabs in place and also to apply pressure while araldite between them was getting dried (Fig. 4.11). Once the sample was dried, paper clamps used to hold tabs in place were removed. Samples were again cured for 5 days before they were put to any testing. A single sample finally would have four tabs (in total) one on either side of both ends. This sample was ready now for any kind of further testing.

### **4.3. TESTING METHODS USED IN EXPERIMENTATION**

#### **4.3.1. Tensile Testing**

A Universal Testing Machine shown in Fig.4.12 and Fig.4.13 was used for the testing of the FRP specimen for its tensile strength. The test specimen had been prepared according to ASTM-D-3039 standard. The specimens were tested until they break indicating the ultimate tensile strength value.



**Fig. 4.12: UTM tensile setup**



**Fig. 4.13: Specimen in jaws**

### 4.3.2. Three Point Flexural Test

Three point bending tests of specimen were carried out in Zwick / Roell machine using the arrangement as shown in fig. 4.14& 4.15.



**Fig. 4.14: UTM flexural setup**



**Fig. 4.15: Specimen positioning**

The test specimen had been prepared according to ASTM-D-790 standard. The three points bending test results can be taken as indications of flexural strength.

### 4.3.3. Micro Hardness Test

Micro hardness test (shown in Fig.4.16) was conducted on specimen with different clay loadings to see the effect of clay loading on hardness values.



**Fig. 4.16: Micro hardness tester**

The load applied was 100 N and VHN values were determined by applying this load by using a calibration distance of 50 units in Quantinets software used for image analyzing. The dwell time used during load application was 20 seconds. An indent was formed in diamond shape used for calculating VHN as shown in figure below.

#### 4.3.4. X-Ray Diffraction Test

**X-ray scattering techniques** are a family of non-destructive analytical techniques which reveal information about the crystallographic structure, chemical composition, and physical properties of materials and thin films. These techniques are based on observing the scattered intensity of an X-ray beam hitting a sample as a function of incident and scattered angle, polarization, and wavelength or energy.

X-ray diffraction was used in this study to investigate the crystallographic structure of the epoxy nanocomposites. XRD will enable the changes that occur to the clay due to the intercalation and/or exfoliation of the epoxy into the clay galleries to be quantified. The d-spacing of the intergallery spacing can be determined using Bragg's Law:

$$\lambda = 2d\sin\theta$$

Where  $\lambda$  is the wavelength of the incidence x-ray source,  $d$  is the spacing in question,  $\theta$  is  $\frac{1}{2}$  of  $2\theta$  the Bragg angle or the diffracted angle of the incidence x-ray beam. Below is a schematic of the previously mentioned Bragg's Law (Fig. 4.17).

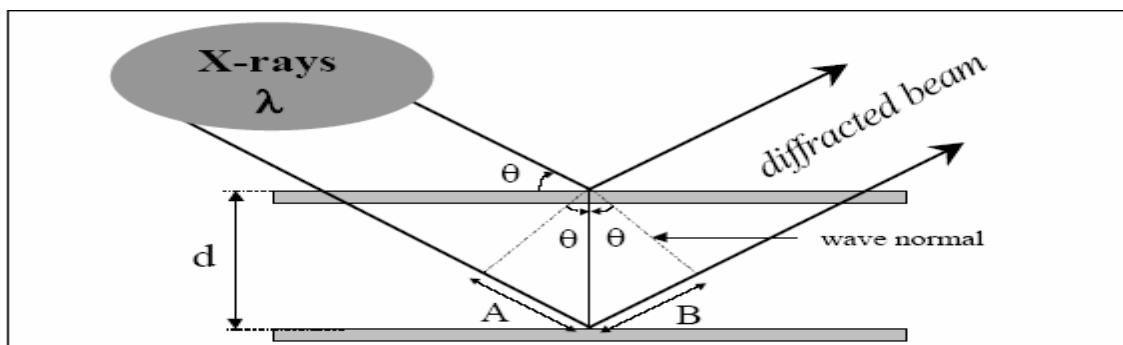


**Fig. 4.17: Schematic representation of x-ray diffraction principle**

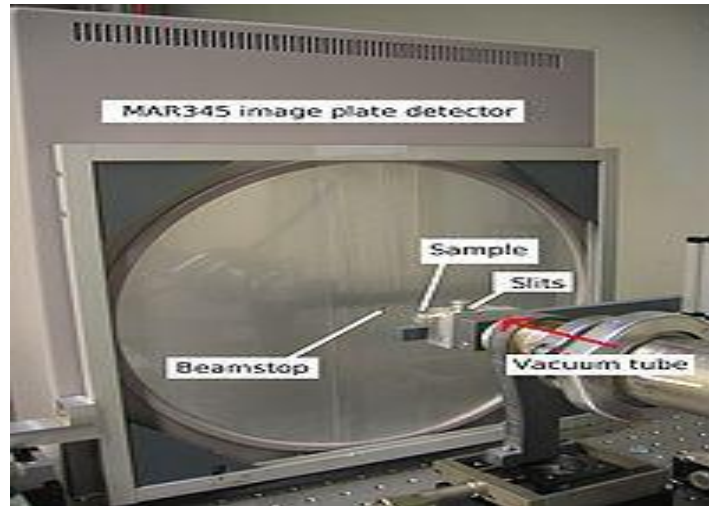


**Fig.4.18: Schematic representation of x-ray diffractometer principle**

To evaluate the degree of exfoliation in the polymer, XRD measurements were carried out in a Panalytical X-ray diffractometer with Cu K $\alpha$  radiation ( $\lambda=1.54\text{\AA}$ ) with a scanning speed of  $1^\circ/\text{min}$  and at 45 kV and 40mA. During the XRD experiments, the samples were analyzed in reflection mode. All XRD scans were through  $2\theta$  of  $3^\circ$  to  $20^\circ$ .

#### 4.3.5. SEM (Scanning Electron Microscope)

Fracture surfaces of laminates were examined with scanning electron microscope (SEM) to investigate the effects of clay addition on the adhesion at the interface between glass fibers and the epoxy matrix, and the extent of clay dispersion. For this purpose, gold vapour deposition was applied onto the fractured surface of tensile specimens to have a conductive layer over the samples.

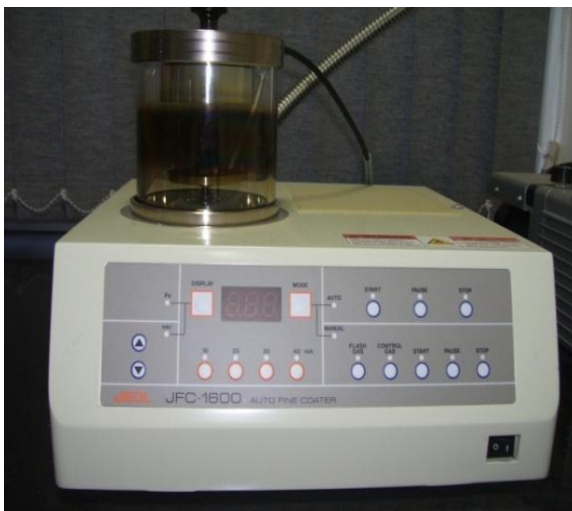


**Fig. 4.19: Gold coating equipment**



**Fig. 4.20: SEM machine**

SEM micrographs are helpful in viewing the micro-structure of material, hence showing any changes in physical structure of material and showing any defects like cracks, voids generated after loading of clay. These are also helpful in calculating the area fraction of fibre and epoxy in the given specimen and the changes occurring and for also calculating the circularity of the fibre in case of GFRP.

**4.3.6. Transmission Electron Microscopy (TEM)** is a vital characterization tool for directly imaging nanomaterials to obtain quantitative measures of particle and/or grain size and morphology.

TEM functions involve four basic operations:

1. A stream of electrons is formed and accelerated towards the specimen using a positive electrical potential,
2. This stream is confined and focused using a metal aperture and magnetic lenses into a thin, monochromatic beam, (magnetic lenses are circular electro-magnets capable of projecting a precise circular magnetic field in a specified region,
3. The focused beam is impinged on the sample by a magnetic lens,
4. The energetic electrons then interact with the irradiated sample. These interactions and effects are detected and transformed into an image.

A schematic of a TEM is illustrated in Figure 4.21.

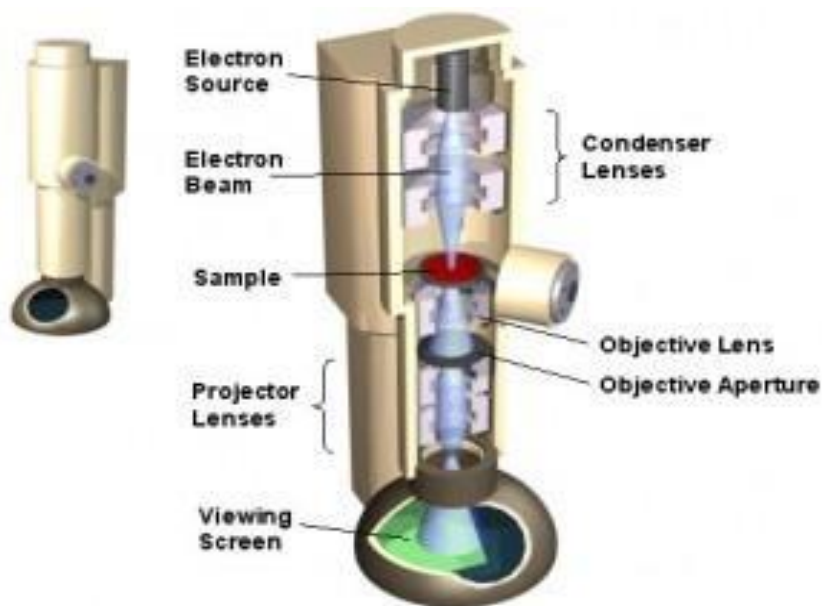


**Fig. 4.21: Schematic of transmission electron microscope**

We used a HITACHI transmission electron microscope operating at an accelerating voltage of 80KV is used in this study to test the morphology and particle size. Sample in powder form is prepared for imaging by drying nanoparticles on a copper grid that is coated with a thin layer of carbon.



## 5.1 MICROSCOPIC BEHAVIOR

### 5.1.1 Micro-Hardness

#### Specimen for Micro Hardness

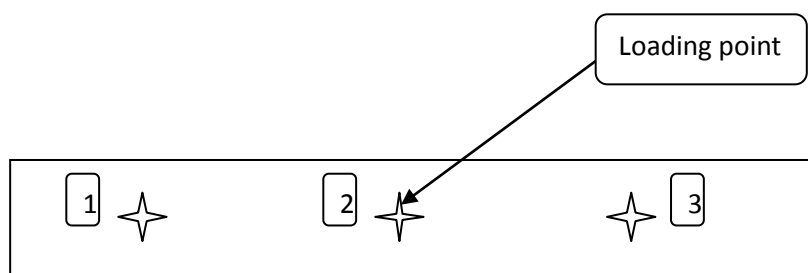


**Fig. 5.1: Indentation in specimen**

The micro-hardness of specimen at different clay loading was measured. The table 5.1 shows the experimental measurements of micro hardness of the nanocomposites with different nanoclay contents. An average hardness was calculated by 3 indentation measurements and a plot of the results of each type of samples is shown in Fig. 5.2.

**Table 5.1: Micro Hardness Values for Different Clay Loading Samples**

Clay loading Loading Points	Micro hardness values (VHN)		
	0%	2%	3%
1 <sup>st</sup> Indent	6.127412	7.365374	6.920115
2 <sup>nd</sup> Indent	5.682314	8.628665	6.920115
3 <sup>rd</sup> Indent	6.610959	7.283413	6.899283
<b>Average</b>	<b>6.140228</b>	<b>7.759151</b>	<b>6.913171</b>

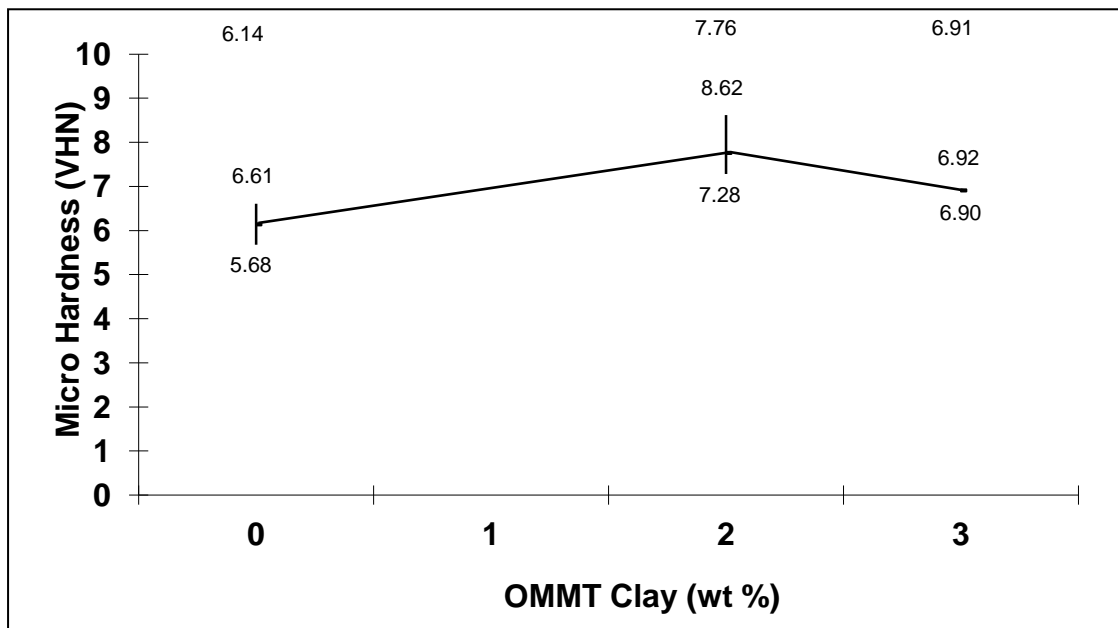


**Fig. 5.2: Micro Hardness test results**

The maximum hardness has been measured where the nanoclay content was 2 wt%. A decline of the hardness is seen on further increasing the nanoclay content. The hardness decreased from 7.759151 VHN (2 wt% of nanoclay) to 6.913171VHN (3 wt% of nanoclay). In most previous literatures, it has been indicated that adding a small amount of nanoclays into polymer-based materials could potentially enhance their strength, hardness of the samples with the nanoclay content less than 3 wt%. The results obtained in the current study show that the microhardness value is dropped if the amount of the nanoclays is beyond 2 wt%.

### 5.1.2 X-ray Diffraction Test

The X-ray diffraction experiments were conducted on the samples having different nanoclayloading. X-ray diffractometer gives the values of d-spacing and  $2\theta$  for different samples of epoxy clay nanocomposites. An increase of the interlayer distance leads to a shift of the diffraction peak toward lower angle. The diffraction peak of Cloisite 30B<sup>®</sup> comes out at an angle  $2\theta = 4.8452^\circ$  having d-spacing value is  $d = 18.26854 \text{ nm}$ , Hence the shift in angle to the lower side shows the increase in d-spacing.

**Table 5.2: d- Spacing of Clay & Epoxy layered silicates**

S.No.	Clay Loading	Angle( $2\theta$ ) in degrees	d- Spacing(nm)
1	Closite 30B	4.8452	18.26854
2	2 wt%	Exfoliation	-----
3	3 wt%	Exfoliation	-----

The characteristics peak of clay as illustrated in fig.5.3 & fig.5.4 is not visible. This may be due to the exfoliation of clay during the polymerization of resin. The exfoliated structure does not show any peak in the X-ray diffractogram. However, the characteristic peaks from any agglomerated clay layers may not be in the detectable level due to the presence of high fraction of glass fibers and epoxy matrix as compared to the fraction of the clays in the composites.

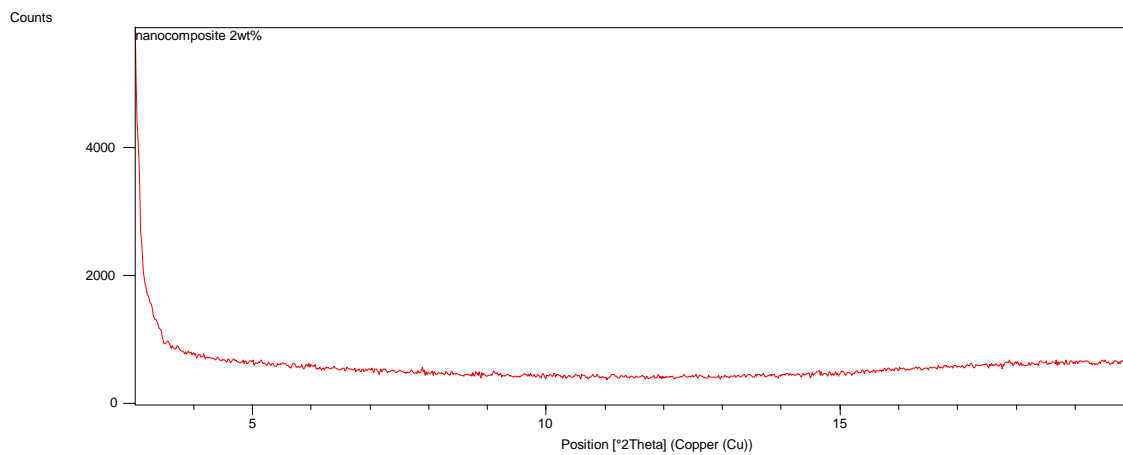


**Fig.5.3: X-ray diffractogram of 2wt% nanoclay**

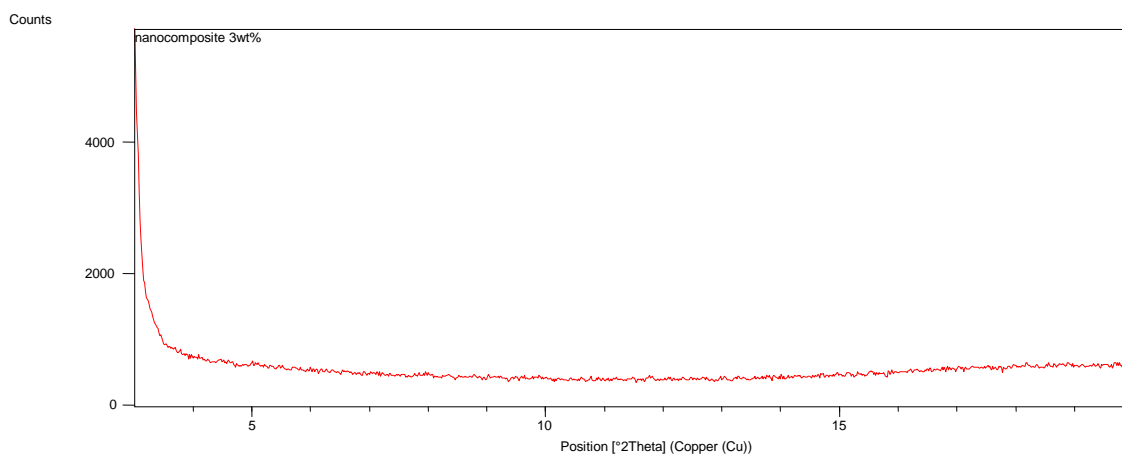


**Fig. 5.4: X-ray diffractogram of 3wt% nanoclay**

### 5.1.3 Scanning Electron Microscopy (SEM)

Figure 5.5 and 5.6 illustrates the SEM fracture surface images of glass fabric reinforced lamina obtained from tensile test specimens prepared with organically modified nanoclay/epoxy suspension. As seen in Fig.5.5 and 5.6, fracture occurs along the interface and smooth fracture surfaces are formed due to weaker interfacial debonding in laminates without clay addition. In contrast, in the case of composites laminated with clay containing epoxy matrix, it is evident that fracture mechanisms are altered due to the presence of clays. The fracture modes indicate that a stronger interface is formed in these composites.

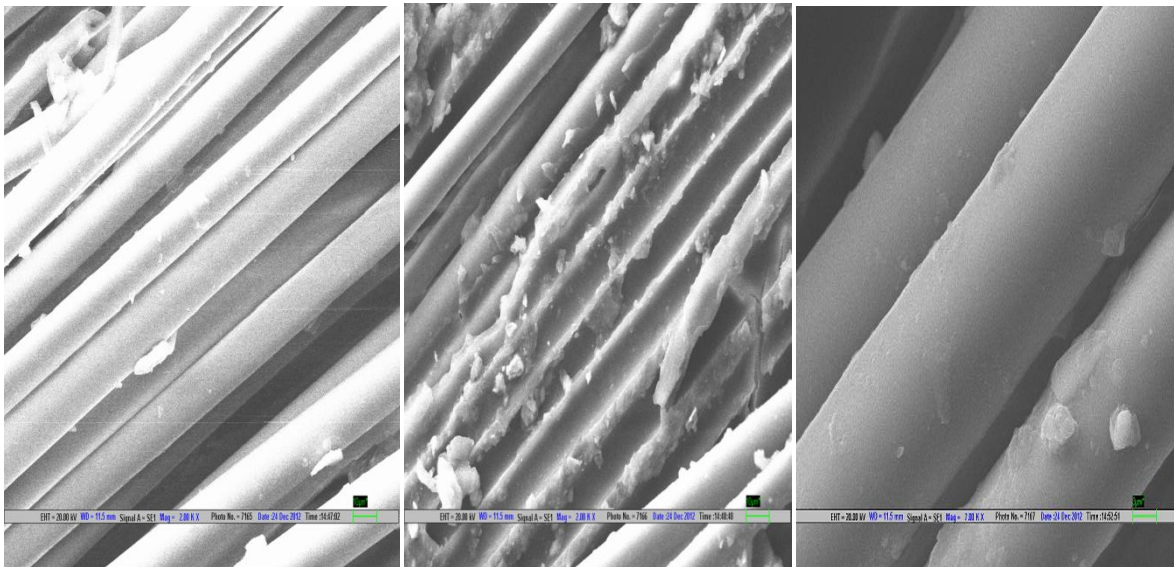


**Fig.5.5: SEM images of fracture surface having 2 wt% nanoclay**

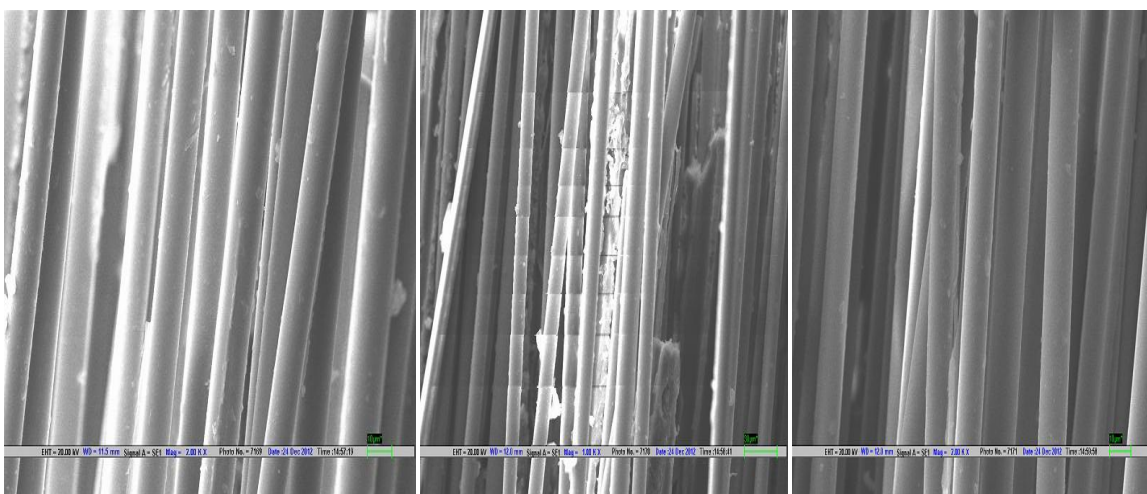


**Fig.5.6: SEM images of fracture surface having 3wt% nanoclay**

### 5.1.4 Transmission electron microscopy (TEM)

Sample in powder form was dissolved in ethanol and sonicated for 1 hour prior to dispersion onto a copper grid using a porous carbon film. The morphological detail of the sample was determined at various magnifications. TEM images, shown in Fig.5.7, 5.8 & 5.9, illustrate the morphology of nanocomposites containing 3wt% clay loadings. The image shows a uniform dispersion of nanoclay particles. The particles appear to be agglomeration-free and the individual particles can be identified very clearly. It shows exfoliated structure and the clay platelets of nanometer thickness dispersed in the polymer matrix are clearly visible.

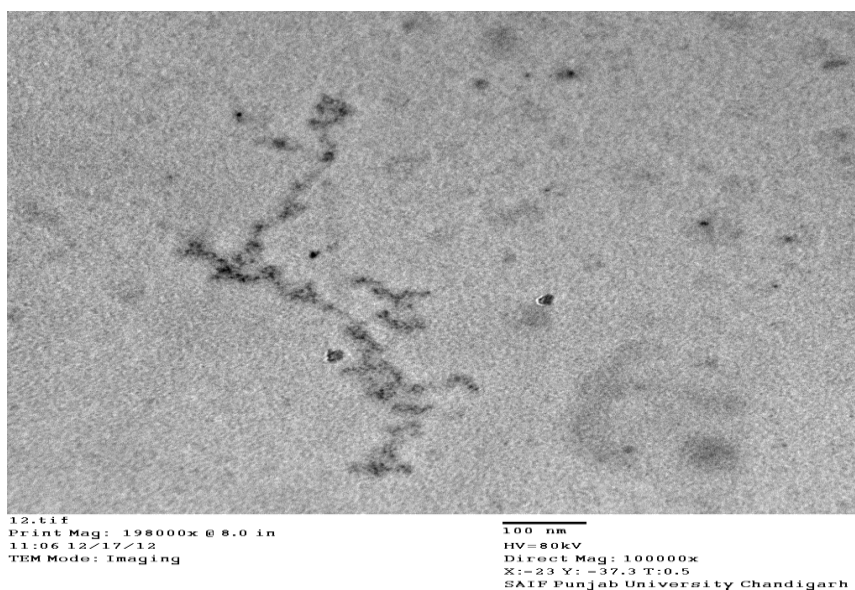


**Fig.5.7: TEM micrograph of 3 wt% nanoclay at 100000 X**

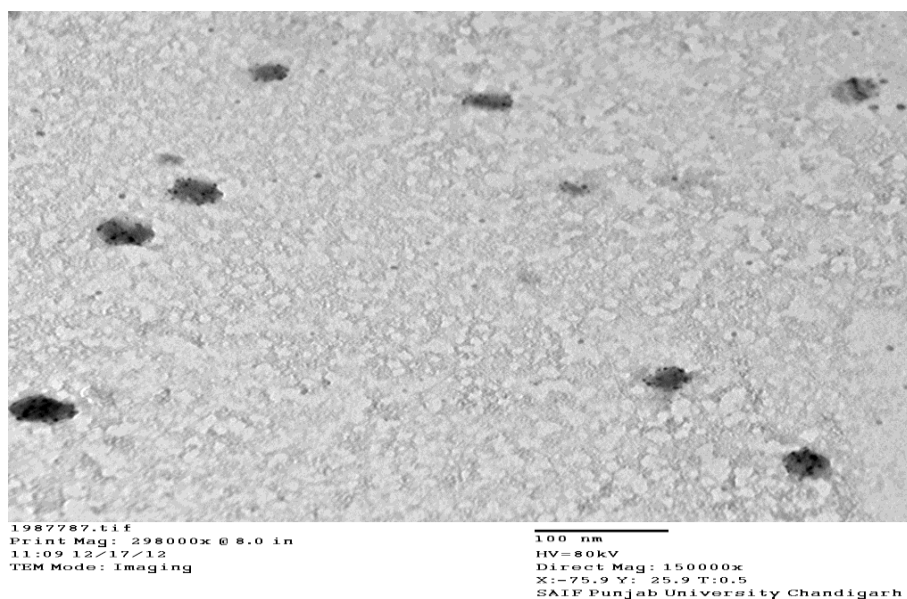


**Fig.5.8: TEM micrograph of 3 wt% nanoclay at 150000 X**

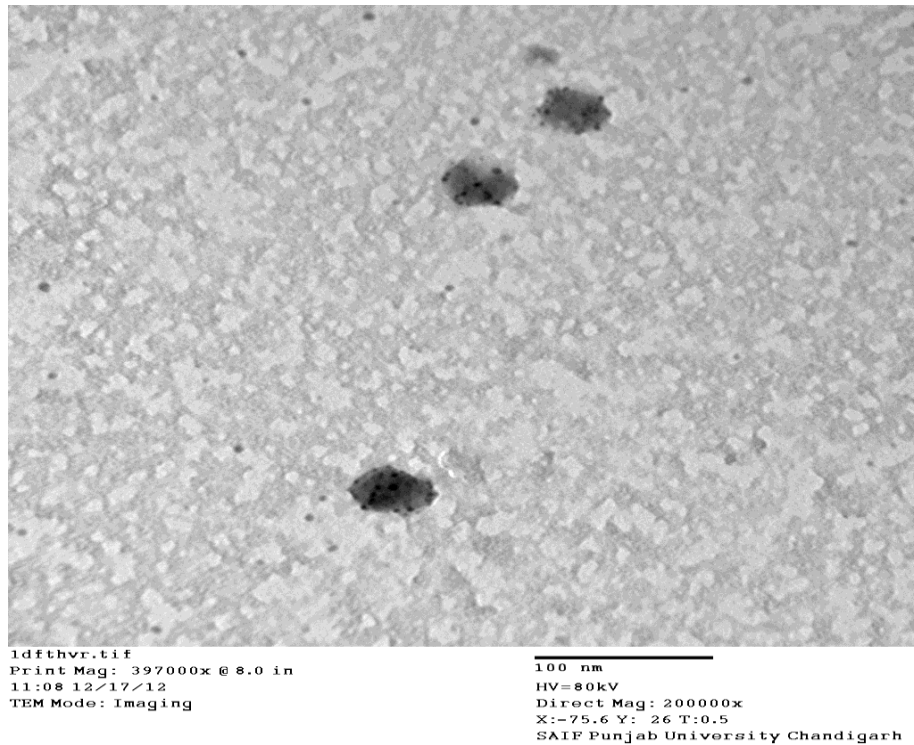


**Fig.5.9: TEM micrograph of 3 wt% nanoclay at 200000 X**

## **5.2 Flexural Behaviour**

The influence of clay loading on the flexural strength of different fiber orientation specimen is as shown in figure 5.10, 5.11, 5.12 & 5.13. Three specimen for each composition, at fiber orientation angles of 30°, 45° and 60° have been tested. Flexural strength increases with the addition of OMMT clay and with the increase in fiber orientation angle. Maximum improvement in flexural strength obtained at 3wt% clay content was 16.80%, 21.80% and 22.62% at fiber orientation angle of 30°, 45° and 60° respectively in comparison to neat epoxy glass fiber specimens. Addition of nanoclay has resulted in improvements of flexural strength in all the specimens. Results indicate that the fiber orientation has also affected the flexural strength. This change may be attributed to the more number of relatively long fibers participating in taking up the bending loads in comparison to short fibers in 30° and 45° specimens.

**Table 5.3: Flexural Strength values of different nanoclaywt % specimen at different fiber orientation angles.**

Nanoclay wt%	Fiber Orientation Angle	Sample No.	Flexural Strength (MPa)	Average Flexural Strength (MPa)
0 wt%	30 <sup>0</sup>	1	138	111.86
		2	99.3	
		3	98.3	
	45 <sup>0</sup>	1	116.5	114.19
		2	92.4	
		3	133.67	
	60 <sup>0</sup>	1	114	118.50
		2	109.5	
		3	132	
2 wt%	30 <sup>0</sup>	1	105	122.34
		2	147.02	
		3	115	
	45 <sup>0</sup>	1	129	128.13
		2	104.4	
		3	154	
	60 <sup>0</sup>	1	132	144
		2	156	
		3	144	
3 wt%	30 <sup>0</sup>	1	138	130.66
		2	130	
		3	124	
	45 <sup>0</sup>	1	103.2	141.06
		2	167	
		3	153	
	60 <sup>0</sup>	1	206	153.10
		2	110.3	
		3	143	

**Table 5.4: Mean flexural strength (MPa) and corresponding percentage increase**

<div style="display: flex; align-items: center;"> <div style="writing-mode: vertical-rl; transform: rotate(180deg);">Fiber Angle(<math>\theta</math>)</div> <div style="margin-left: 20px;">                     Nanoclay loading(wt %)                     <div style="display: flex; align-items: center; margin-top: 5px;"> <span style="font-size: 2em; margin-right: 10px;">↔</span> <span style="font-size: 2em;">↔</span> </div> </div> </div>	0 wt%	2 wt%	3 wt%	Percentage increase in flexural strength of 2 wt% loading	Percentage increase in flexural strength of 3 wt% loading
$30^{\circ}$	111.86	122.34	130.66	8.56%	16.80%
$45^{\circ}$	114.19	128.13	141.06	10.87%	21.80%
$60^{\circ}$	118.5	144	153.1	17.70%	22.62%

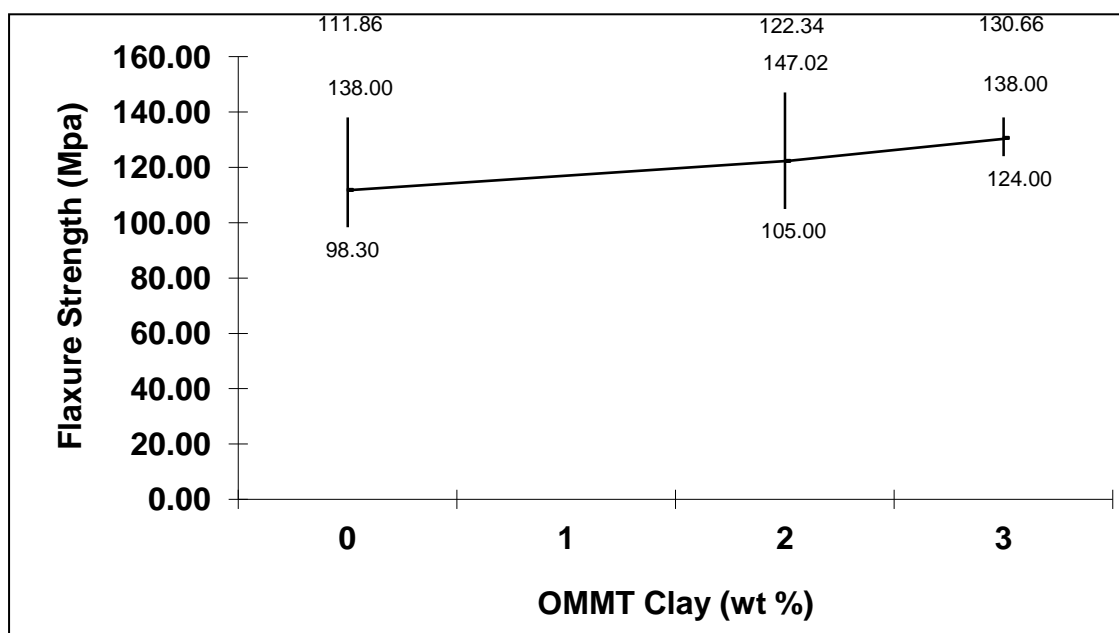


**Fig 5.10: Flexure Strength vs Nanoclay wt % ( $30^{\circ}$  angle)**

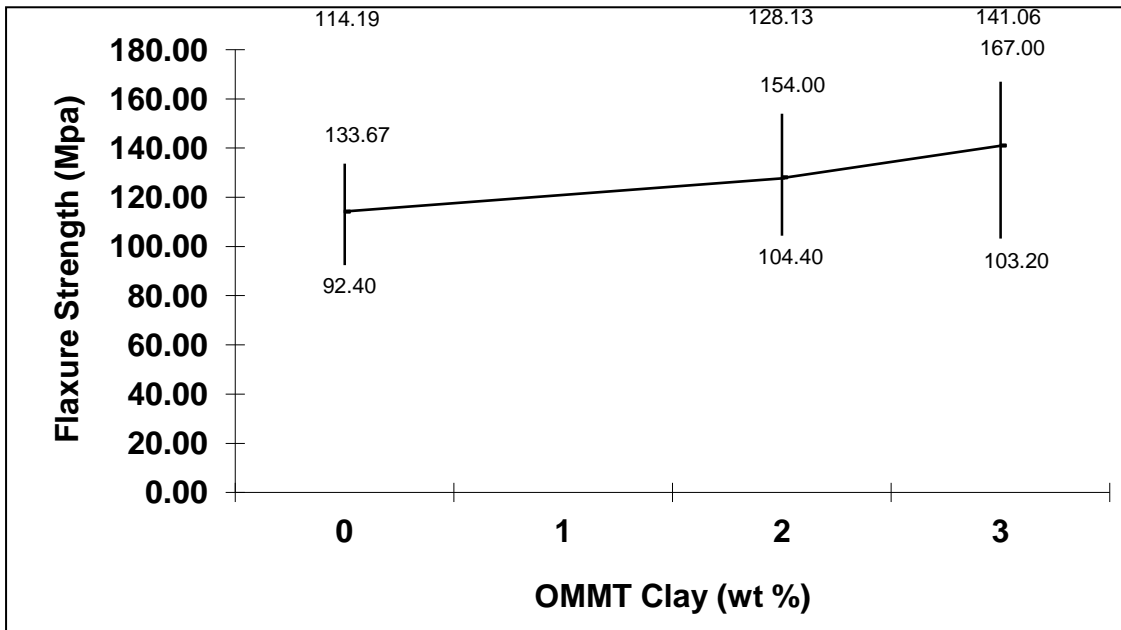


Fig 5.11: Flexure Strength vs Nanoclay wt % (45° angle)

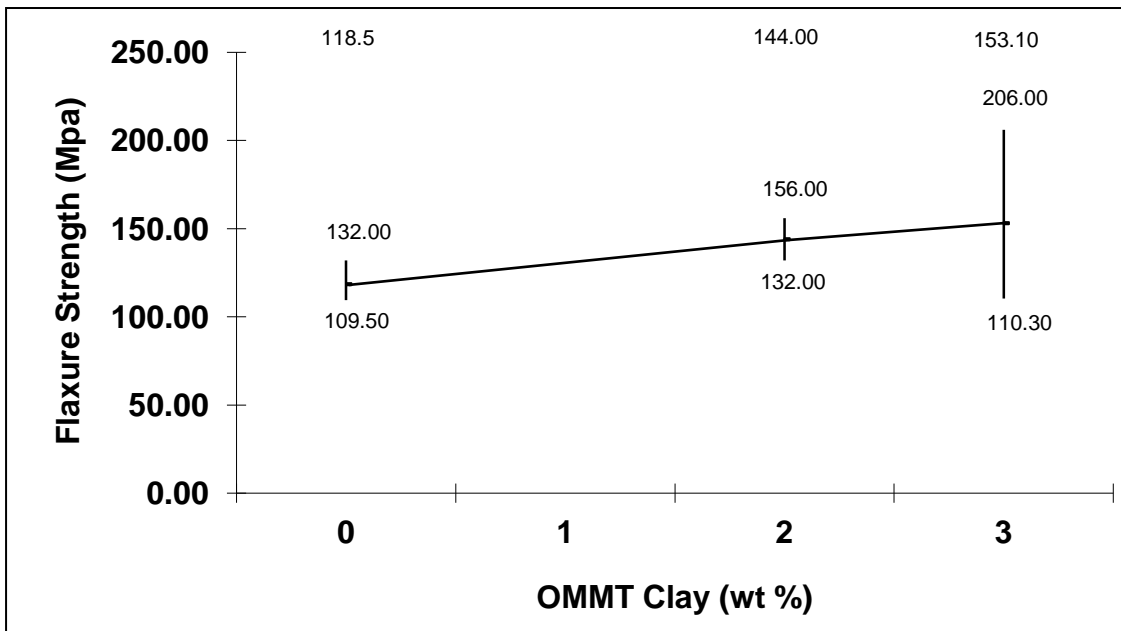
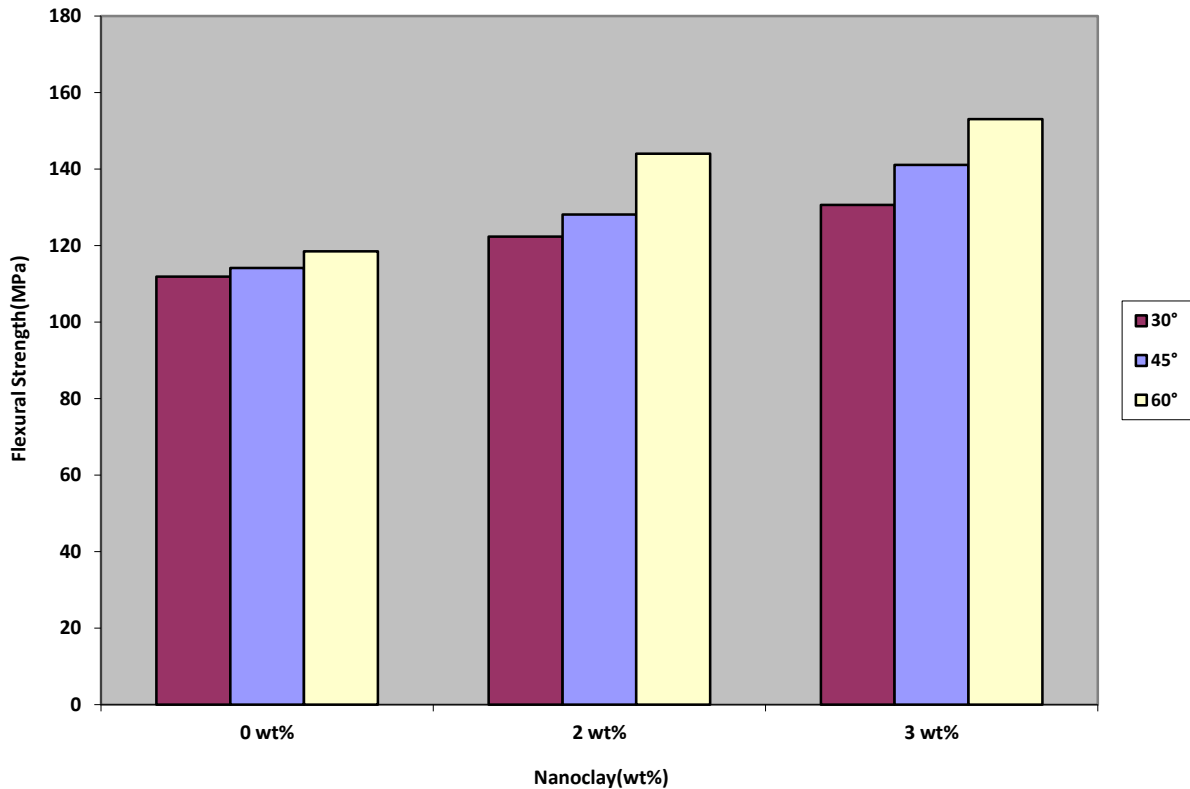


Fig 5.12: Flexure Strength vs Nanoclay wt % (60° angle)



**Fig. 5.13 Flexural strength of Epoxy/Glass Fiber, 2 wt% Nanoclay/Epoxy/Glass Fiber and 3 wt% Nanoclay/Epoxy/Glass Fiber at different fiber orientation.**

### 5.3 Tensile Behaviour

Tensile tests were performed on the fiber reinforced composite to observe the effect of modified clay addition to the matrix resin on the tensile behaviour of composite. Figure 5.14, 5.15, 5.16 & 5.17 exhibits the tensile strength of the different nanoclay loading specimen at different fiber orientation angle. Maximum increase in tensile strength is observed at 3wt% nanoclay addition. 10.44%, 8.22% and 10.57% increase in the tensile strength values at fiber orientation angle of 30<sup>0</sup>, 45<sup>0</sup> and 60<sup>0</sup> respectively have been observed as compared to those fabricated with neat epoxy. The result indicates that modifying the matrix resin of glass reinforced epoxy composite with clay has influenced the tensile properties of the lamina due to exfoliation of nanoclay in matrix resin. Improvement in the tensile strength may be attributed to a mechanical interlocking effect provided by nanoclay, like micro-pins inside the matrix environment.

**Table: 5.5: Tensile Strength values of different nanoclaywt % specimen at different fiber orientation angles.**

Nanoclay wt%	Fiber Orientation Angle	Sample No.	Tensile Strength (MPa)	Average Tensile Strength (MPa)
0 wt%	30 <sup>0</sup>	1	64.4	54.26
		2	47.8	
		3	50.6	
	45 <sup>0</sup>	1	51.9	50.73
		2	53.8	
		3	46.5	
	60 <sup>0</sup>	1	66	56.46
		2	64.7	
		3	38.7	
2 wt%	30 <sup>0</sup>	1	65.2	57.73
		2	56.8	
		3	51.2	
	45 <sup>0</sup>	1	62.5	52.46
		2	59	
		3	37.1	
	60 <sup>0</sup>	1	60.4	60.16
		2	57.8	
		3	62.3	
3 wt%	30 <sup>0</sup>	1	51.3	59.93
		2	64.7	
		3	63.8	
	45 <sup>0</sup>	1	58.9	54.9
		2	52.8	
		3	53.1	
	60 <sup>0</sup>	1	63.3	62.43
		2	62.5	
		3	61.5	

**Table 5.6: Mean tensile strength (MPa) and corresponding percentage increase**

Nanoclay loading (wt%) Fiber Angle( $\theta$ )	0 wt%	2wt%	3wt%	Percentage increase in tensile strength of 2 wt% loading	Percentage increase in tensile strength of 3 wt% loading
	$30^0$	54.26	57.73	59.93	6.39%
$45^0$	50.73	52.86	54.90	4.19%	8.22%
$60^0$	56.46	60.16	62.43	10.46%	10.57%

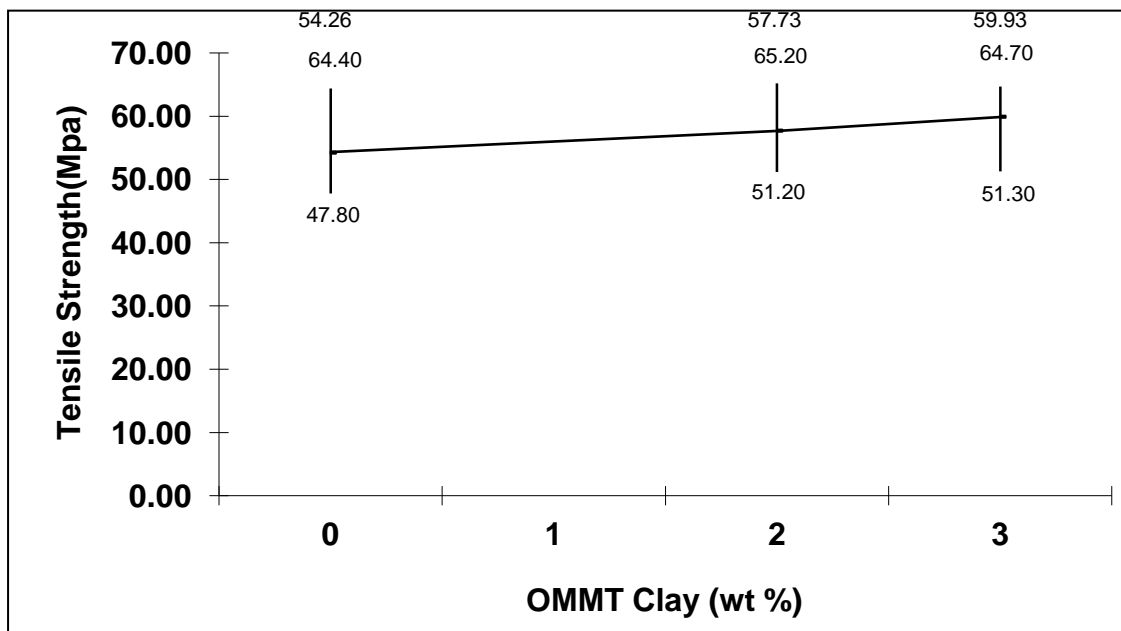


**Fig 5.14: Tensile Strength vs Nanoclay wt % ( $30^{\circ}$  angle)**

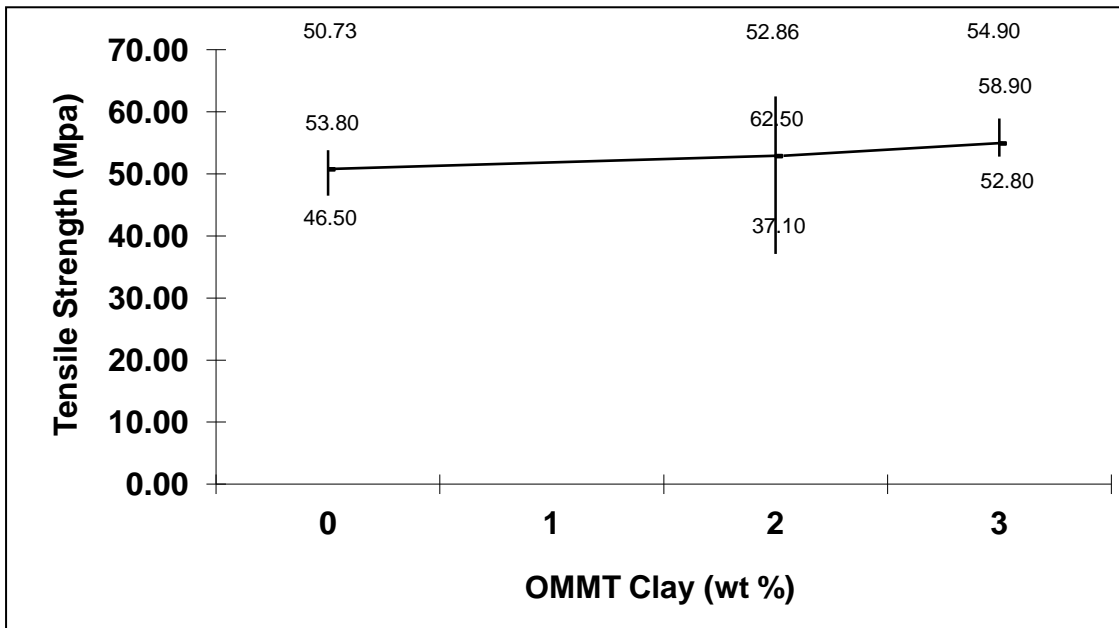


**Fig 5.15: Tensile Strength vs Nanoclay wt % (45° angle)**

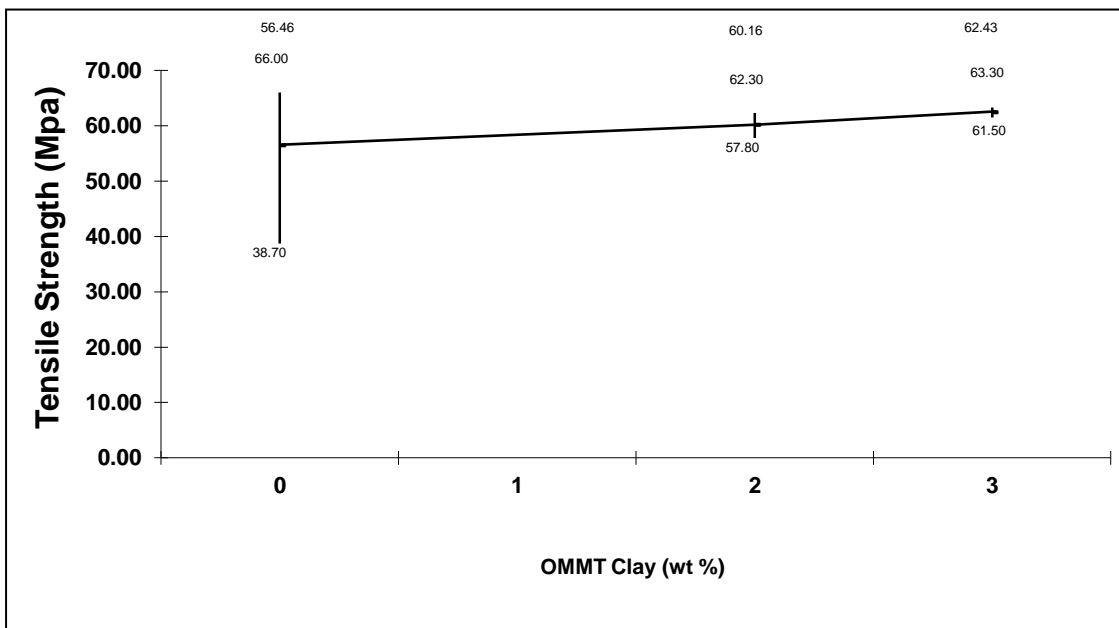


**Fig 5.16: Tensile Strength vs Nanoclay wt % (60° angle)**

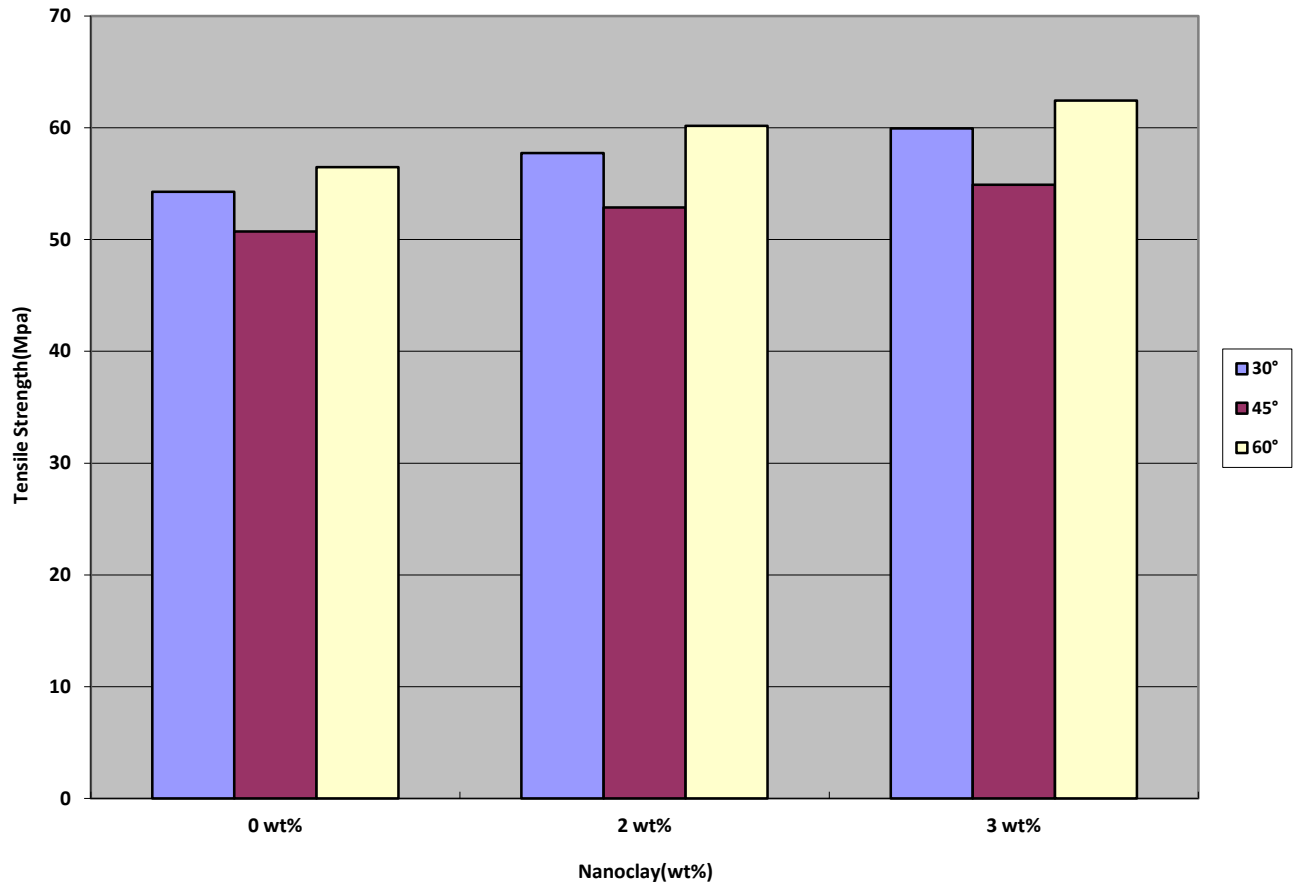


**Fig. 5.17: Tensile strength of Epoxy/Glass Fiber, 2 wt% Nanoclay/Epoxy/Glass Fiber and 3 wt% Nanoclay/Epoxy/Glass Fiber at different fiber orientation.**

**6.1 CONCLUSION**

Glass fiber reinforced epoxy nanoclay composites have been synthesized using hand layup method. TEM micrographs showed exfoliation of nanoclay at 2 wt% and 3 wt% in epoxy. The absence of diffraction peaks in X- ray diffratograms also indicate exfoliation. Microhardness of the nanocomposites increased with increasing nanoclay content upto 2 wt%. The flexural strength and tensile strength increased with the addition of nanoclay and also with the increase in fiber orientation angle. Maximum improvement in flexural strength and tensile strength are obtained at 3wt% nanoclay loading and by the addition of nanoparticles the flexural strength and tensile strength are improved by 22.62% and 10.57% respectively.

**6.2 FUTURE SCOPE**

1. Experiments may be performed on laminates by stacking unidirectional glass fiber at different angle orientation.
2. To see the effect of nanofillers on FRP's, experiments can be repeated by changing the type of nanofillers.

## REFERENCES

---

**BetimeNuhiji, Darren Attard, Gordon Thorogood, Tracey Hanley, Kevin Magniez, Bronwyn Fox (2011)**, “The effect of alternate heating rates during cure on the structure property relationships of epoxy/MMT clay nanocomposites”, *Composite Science and Technology* 71(2011) 1761-1768

**EmrahBozkurt, Elcin Kaya, MetinTanoglu(2007)**, “Mechanical and thermal behaviour of non-crimp glass fiber reinforced layered clay/epoxy nanocomposites”, *Composites Science and Technology* 67 (2007) 3394–3403

**IsilIsik, UlkuYilmazer and GoknurBayram (2003)**, “Impact modified epoxy / montmorillonitenanocomposites: synthesis and characterization”, *Polymer*, 44, 6371–6377.

**Jinwei Wang, ShuchaoQin(2007)**, “Study on the thermal and mechanical properties of epoxy–nanoclay composites: The effect of ultrasonic stirring time”, *Materials Letters* 61 (2007) 4222–4224

**Klaus D. Sattler<sup>[1]</sup>**, *Handbook of Nanophysics*, CRC press, ISBN- 978-1-4200-7552-6

**L. Aktas and M. C. Altan(2010)**, “Effect of nanoclay content on properties of glass–waterborne epoxy laminates at low clay loading”, *Materials Science and Technology* 2010 VOL 26 NO 5

**Li-Yu Lin, Joong-Hee Lee, Chang-Eui Hong, Gye-HyoungYoo, Suresh G. Advani(2006)**, “Preparation and characterization of layered silicate/glass fiber/epoxy hybrid nanocomposites via vacuum-assisted resin transfer molding (VARTM)” *Composites Science and Technology* 66 (2006) 2116–2125

**Mahmood M Shokriea, Mohammad A Torabizadeh&AbdolhosseinFereidoon(2011)**, “Dynamic failure behaviour of glass/epoxy composites under low temperature using Charpy impact test method”, *Indian Journal of Engineering & Materials Sciences* Vol. 18, June 2011, pp. 211-220

**Manjunatha C.M, Taylor A.C, Kinloch A.J and Sprenger S, (2009)**, “The tensile fatigue behaviour of a silica nanoparticle-modified glass fiber reinforced epoxy composites”, *Composite science and technology*, 70, 193-199.

**Mo-lin Chan, Kin-tak Lau, Tsun-tat Wong, Mei-poHo, David Hui(2011)**, “Mechanism of reinforcement in a nanoclay/polymer composite”, *Composites: Part B* 42 (2011) 1708–1712

**Marino Quaresimin, Marco Salviato, Michele Zappalorto(2011)**, “Fracture and interlamellar properties of clay-modified epoxies and their glass reinforced laminates”, Engineering Fracture Mechanics 81 (2012) 80–93

**Quang T. Nguyen, Donald G. Baird<sup>[2]</sup>(2007)**, “Preparation of Polymer–Clay Nanocomposites and their Properties”, 2007 Wiley Periodicals, Inc. AdvPolymTechn 25: 270–285, 2006

**Sinha R. S., Okamoto M., (2003)**, “Polymer/layered silicate nanocomposites: a review from preparation to processing”. Prog.Polym. Sci., 28, 1539–1641.

**WitchudaDaud, Harald E.N. Bersee, Stephen J. Picken, AdriaanBeukers(2009)** “Layered silicates nanocomposite matrix for improved fiber reinforcedcomposites properties”, Composites Science and Technology 69 (2009) 2285–2292

**W. S. Chow(2007)**, “Water absorption of epoxy/glass fiber/organo-montmorillonitenanocomposites”, eXPRESS Polymer Letters Vol.1, No.2 (2007) 104–108

**Zainuddin S, Hosur M.V, Zhou Y, Kumar Ashok and Jeelani S, (2010)**, “Durability study of neat/nanophased GFRP composite subjected to different environmental conditioning”, Material science and engineering, A 57, 3091-3099.

**N. Salahuddin a,\* , A. Moet b, A. Hiltner c, E. Baer c (2001)**, European Polymer Journal 38 (2002) 1477–1482